Stratigraphic evolution and characteristics of lobes: a high-resolution study of Fan 3, Tanqua Karoo, South Africa.

by

J.M. Neethling

Thesis presented in partial fulfilment of the requirements for the degree of

Master of Science

at the University of Stellenbosch

Supervisors

Dr. H. de V. Wickens

Dr. D.M. Hodgson

March 2009

Geology

Stellenbosch University

Appendix B

PetroSA Presentation

PetroSA Presentation

The presentation was given as per agreement with PetroSA for the aid provided with the modelling section of this project.

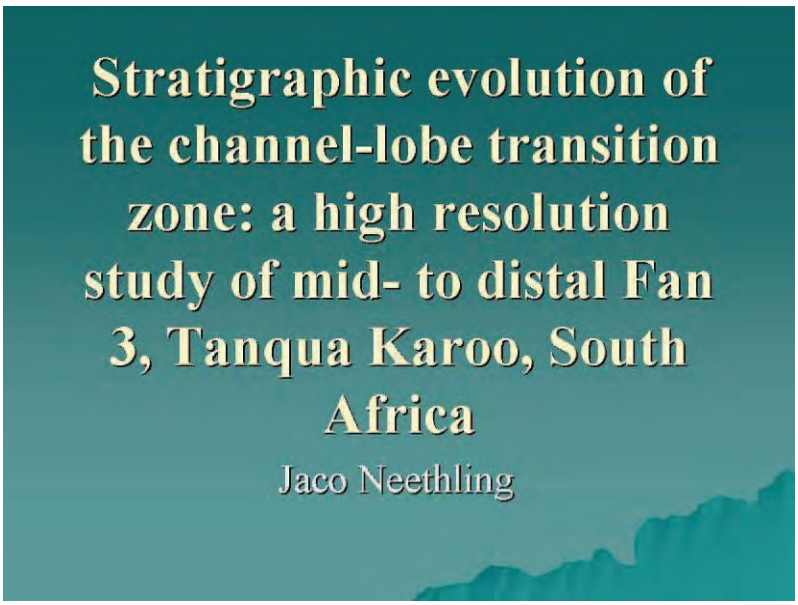

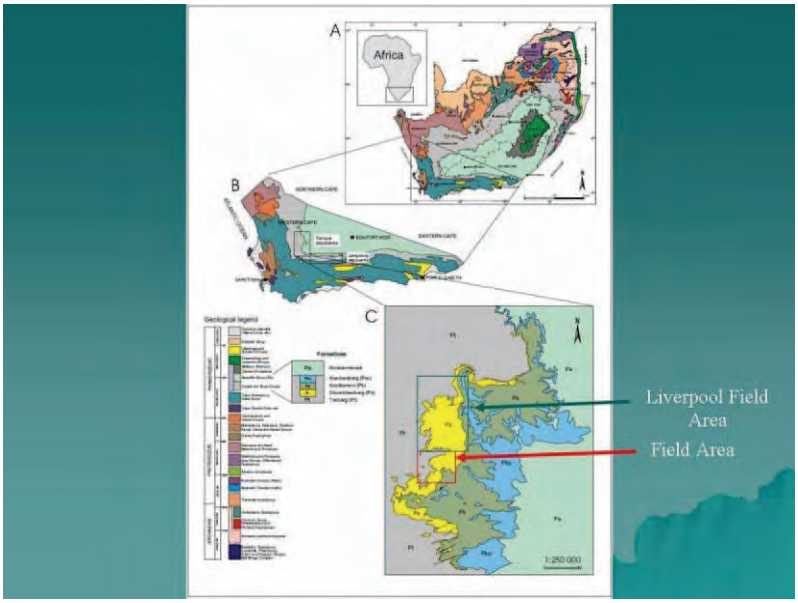

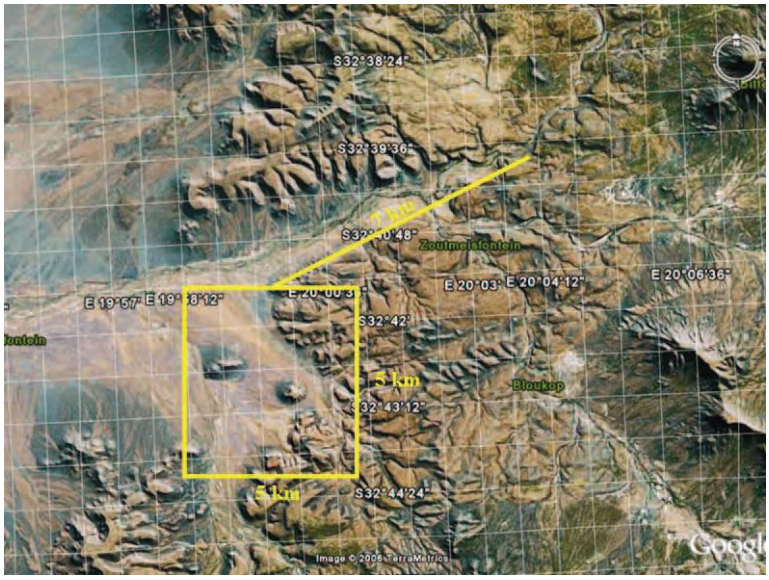
S32°38'24"
S32°39'36"
S32°40'48"
Zoutmeisfontein
E 19°57'
E 19°58'12"
E 20°00'
E 20°03'
E 20°04'12"
E 20°06'36"
S32°42'
5 km
5 km
S32°43'12"
S32°44'24"
Bloukop
Image © 2006 TerraMetrics

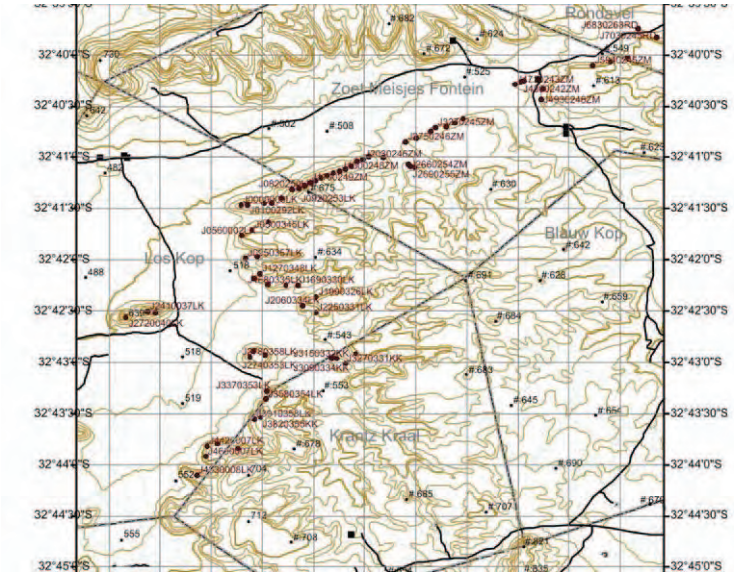
Rondavel
Zoet Vleisjes Fontein
Blauw Kop
Los Kop
Kranz Kraal
32°40'0"S
32°40'30"S
32°41'0"S
32°41'30"S
32°42'0"S
32°42'30"S
32°43'0"S
32°43'30"S
32°44'0"S
32°44'30"S
32°45'0"S

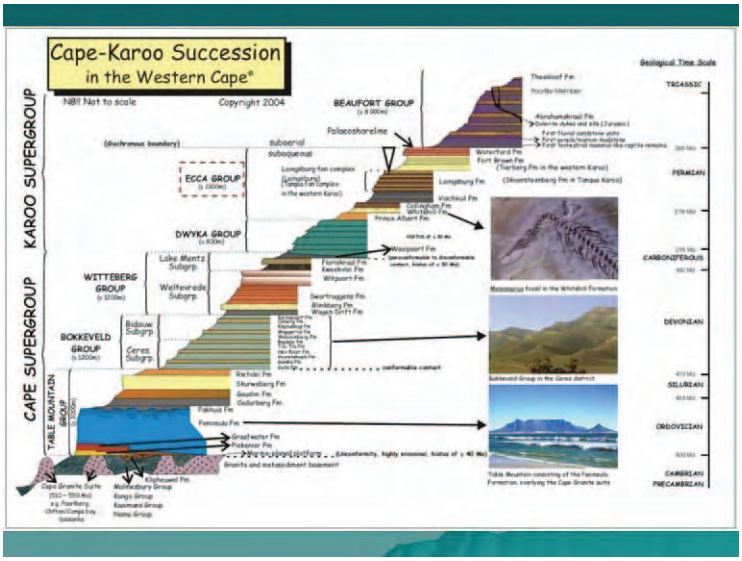
Cape-Karoo Succession
in the Western Cape*
NB!! Not to scale
Copyright 2004
KAROO SUPERGROUP
CAPE SUPERGROUP
BEAUFORT GROUP
ECCA GROUP
DWYKA GROUP
WITTEBERG GROUP
BOKKEVELD GROUP
TABLE MOUNTAIN GROUP
Palaeoshoreline
Geological Time Scale
TRIASSIC
PERMIAN
CARBONIFEROUS
DEVONIAN
SILURIAN
ORDOVICIAN
CAMBRIAN
PRECAMBRIAN

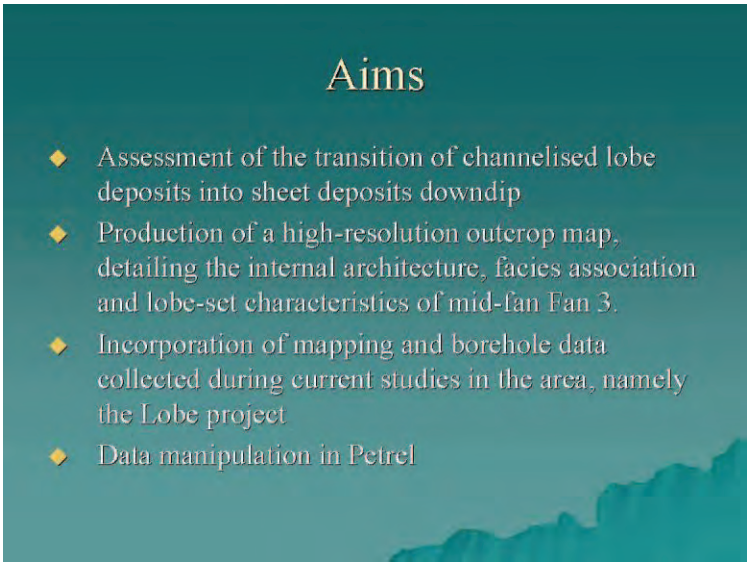
Aims
Assessment of the transition of channelised lobe deposits into sheet deposits downdip
Production of a high-resolution outcrop map, detailing the internal architecture, facies association and lobe-set characteristics of mid-fan Fan 3.
Incorporation of mapping and borehole data collected during current studies in the area, namely the Lobe project
Data manipulation in Petrel

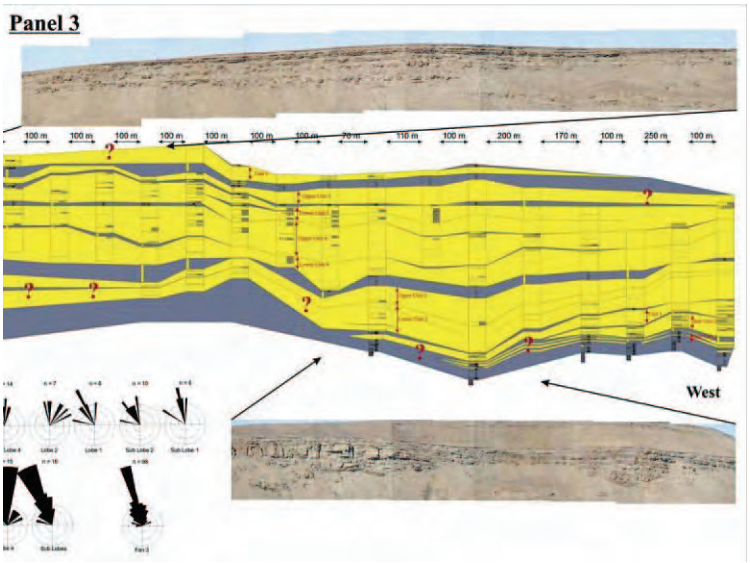
Panel 3
West


Structureless Sandstone

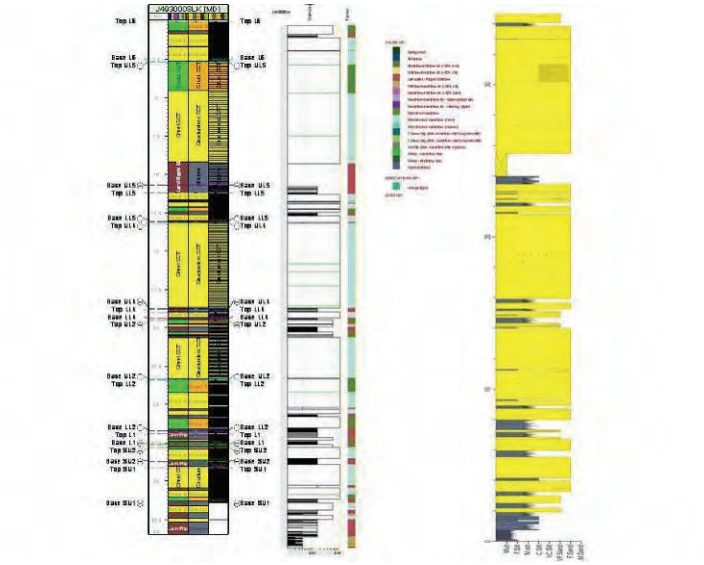

Profile Name	X Coordinate	Y Coordinate	Top	Top L6	Base L6	Top UL5	Base UL5	Top LL5	Base LL5	Top UL4	Base UL4	Top LL4	Base LL4	Top UL2	Base UL2	Top LL2
J7000245RD	412255	6395590	550	566.00	559.95	566.31	560.31	557.77	555.91	554.66	552.66	552.36	552.36	552.16	552.16	551.96
J6502053RD	411967	6395745	551	563.30	561.40	561.20	561.20	561.00	559.63	559.53	556.90	556.76	556.76	556.56	556.56	555.36
J6450245RD	411517	6395294	555	566.00	562.51	561.45	561.45	560.41	578.55	579.24	576.59	575.49	575.49	575.29	575.29	575.09
J6160245ZM	411553	6395156	550	563.00	560.80	560.00	560.00	560.19	563.59	563.39	561.39	561.19	561.19	560.99	560.99	560.79
J5960245ZM	411283	6395093	552	561.30	574.19	573.15	573.15	572.18	570.29	569.69	567.69	567.49	567.49	567.29	567.29	567.09
J6002462M	410522	6394951	557	557.00	552.28	561.73	561.73	561.18	557.68	557.38	554.63	554.43	554.43	554.43	554.43	554.23
J4930245ZM	410488	6394955	576	576.00	571.03	570.50	570.50	569.96	565.84	565.12	562.94	562.14	562.14	561.94	561.94	561.74
J4902462M	410236	6394795	559	559.20	556.40	558.20	558.20	558.00	551.16	550.46	548.74	548.54	548.54	548.34	548.34	548.14
J4900245ZM	410161	6394775	560	560.00	559.20	559.80	559.80	559.59	553.91	553.47	547.79	547.59	547.59	547.39	547.39	547.19
J4710245M	410103	6394732	560	562.30	560.40	560.20	560.20	560.00	556.07	555.63	551.31	551.11	551.11	550.91	550.91	550.71
J3730245ZM	409310	6394105	567	567.00	564.05	563.63	563.63	563.00	558.64	558.04	553.32	553.12	553.12	552.92	552.92	552.72
J3670245ZM	409265	6394023	572	572.00	569.79	569.41	569.41	569.02	565.24	564.79	559.67	559.54	559.32	559.12	559.12	557.92
J3430245ZM	409052	6393951	568	568.00	564.74	564.05	564.05	563.26	559.62	559.02	552.30	552.11	550.21	550.01	549.18	549.09
J3270245ZM	408888	6393941	571	571.00	570.36	569.95	569.95	569.54	564.74	564.11	557.76	556.89	556.32	555.46	553.09	552.67
J3160245ZM	408816	6393872	569	571.20	569.40	569.20	569.20	569.00	565.26	564.66	556.76	556.76	553.66	553.16	550.36	550.36
J2920245ZM	408596	6393745	563	567.40	565.50	565.30	565.30	565.10	563.20	563.00	557.59	556.67	554.32	553.02	549.71	549.64
J2760245ZM	408578	6393217	550	550.00	548.34	548.30	548.30	548.26	544.96	544.96	539.66	539.66	538.33	538.23	534.76	534.66
J2750245ZM	408406	6393602	565	569.40	567.50	567.30	567.30	567.10	565.20	565.00	563.59	563.00	559.76	559.66	555.62	555.46
J2690255ZM	408512	6393242	555	557.30	555.40	555.20	555.20	555.00	550.90	550.28	546.38	545.38	542.50	542.24	539.73	539.53
J2660254ZM	408462	6393272	552	556.40	554.50	554.30	554.30	554.10	552.20	552.00	546.69	546.69	546.66	544.95	542.99	542.19
J2340245ZM	408094	6393398	576	580.40	578.50	578.30	578.30	578.10	576.20	576.00	572.41	570.74	567.68	564.97	562.50	562.50
J2150246ZM	407972	6393410	569	591.10	589.20	589.00	589.00	589.11	585.24	584.76	581.77	581.67	577.67	575.68	572.04	571.84
J2000246ZM	407788	6393353	593	593.00	592.22	591.18	590.35	589.86	587.65	587.03	582.87	582.49	579.07	576.62	574.18	574.18
J1930246ZM	407570	6393315	601	601.00	599.41	598.21	597.55	597.08	594.00	593.16	589.97	589.64	585.34	582.92	580.66	580.12
J1800247ZM	407506	6393220	607	607.00	605.30	603.68	602.75	602.00	598.98	598.28	596.21	595.64	592.04	591.04	590.74	590.64
J1700248ZM	407517	6393184	602	604.10	602.20	602.00	601.72	601.35	597.45	597.09	594.10	593.86	588.25	588.05	589.95	589.75
J1600249ZM	407427	6393149	609	611.80	609.70	609.50	609.02	609.00	604.49	603.89	599.68	599.08	595.22	595.02	596.92	596.72
J1500248ZM	407332	6393110	617	619.10	617.20	617.00	616.31	616.11	613.01	612.46	606.62	606.42	600.22	600.12	610.03	609.83
J1400247RM	407237	6393062	626	628.20	626.30	626.10	622.74	622.20	619.10	618.57	613.95	613.78	611.51	608.81	607.61	607.56
J1300248ZM	407140	6393021	630	632.30	630.54	629.70	629.00	629.50	624.41	624.41	620.62	620.62	618.02	618.72	617.20	617.20
J1200249ZM	407058	6392957	636	636.00	634.55	633.59	631.69	631.23	629.15	629.15	623.05	623.56	621.95	621.65	623.95	623.35
J1100249ZM	406994	6392900	637	637.00	635.10	635.10	632.72	632.52	630.98	630.68	629.00	629.00	623.76	623.76	619.26	619.16
J1000252ZM	406903	6392875	635	635.00	634.10	632.97	630.51	630.16	627.46	627.46	622.16	622.16	619.33	617.78	615.19	615.19
J0920253LK	406808	6392816	625	625.00	624.20	623.04	620.14	619.95	615.30	615.20	610.55	610.35	612.25	612.05	612.95	612.75
J0820250LK	406709	6392801	622	621.52	620.56	619.52	616.22	616.01	612.11	611.88	606.97	606.67	600.72	602.54	598.30	598.30
J0620258LK	406552	6392653	626	626.00	625.00	625.80	623.76	622.84	618.69	618.65	617.15	616.95	612.86	611.42	609.52	608.52
J0450258LK	406396	6392568	616	618.30	616.30	616.10	616.20	616.00	611.97	611.97	609.33	609.13	605.98	604.65	602.35	602.35
J0350259LK	406277	6392534	615	619.40	619.40	619.20	617.30	617.10	615.20	615.00	612.20	612.20	608.80	607.50	604.66	604.66
J0100292LK	406026	6392520	623	625.30	625.30	625.10	623.20	623.00	622.48	622.23	619.89	619.69	616.80	616.80	614.67	614.67
J0000003LK	405803	6392519	625	626.20	626.20	626.00	624.45	624.33	622.31	622.31	620.41	620.41	616.31	615.81	613.71	613.71
J0500312LK	405510	6392215	574	576.40	576.40	576.20	576.30	576.10	574.30	574.00	570.64	570.64	570.42	569.92	567.58	567.58
J0950002LK	405248	6391957	604	606.30	606.30	606.10	604.20	604.00	600.22	600.02	596.66	596.66	596.14	597.14	594.74	594.74
J0500345LK	406102	6392059	596	600.30	600.30	600.10	598.20	598.00	591.96	591.96	589.96	589.96	588.16	587.11	586.09	585.93
J0950345LK	406166	6391605	595	597.10	595.20	595.00	593.00	592.83	573.78	577.04	569.96	570.16	571.28	571.08	568.04	565.74
J0950357LK	406006	6391555	576	576.10	575.20	576.00	574.05	573.92	566.88	570.16	564.33	567.53	566.63	565.48	569.46	559.81
J1270348LK	406227	6391298	578	582.20	580.30	580.10	578.20	579.00	576.51	576.51	573.49	573.49	571.40	569.89	566.94	566.54
J1300352LK	406146	6391193	579	582.20	580.30	580.10	578.20	578.00	572.01	573.16	569.16	571.75	569.66	569.65	567.55	567.37
J1490345LK	406359	6391089	583	587.20	585.30	585.10	583.20	583.00	581.74	581.61	578.13	579.13	577.42	575.28	572.05	571.85

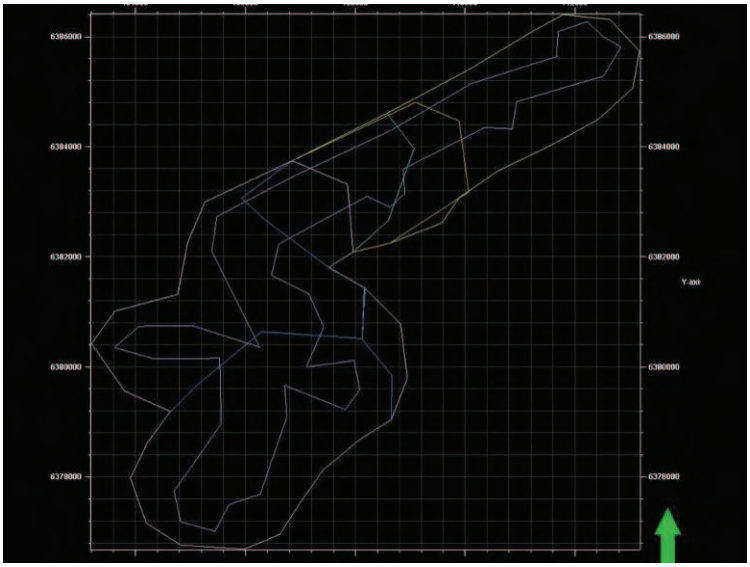

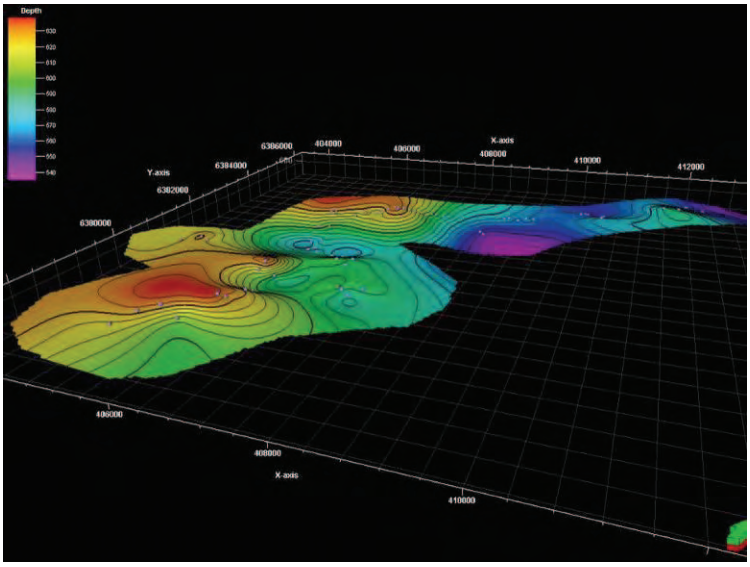
Depth
X-axis
Y-axis
404000
406000
408000
410000
412000
6386000
6384000
6382000
6380000

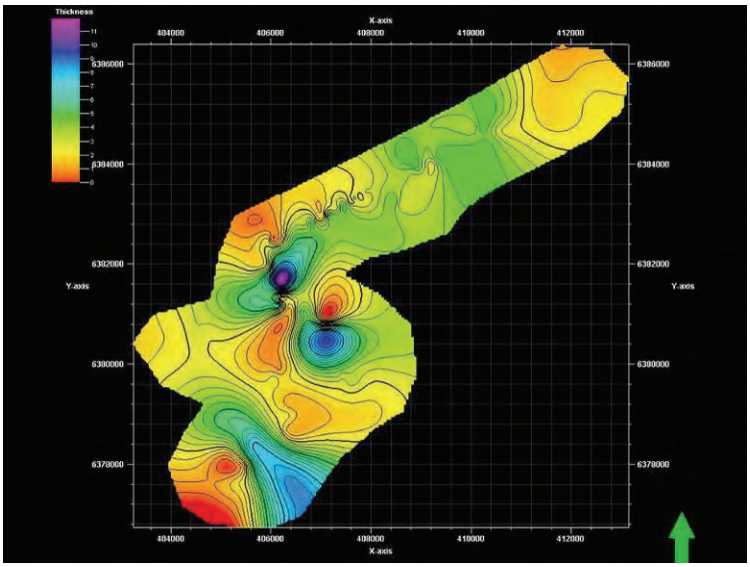
Thickness
X-axis
Y-axis
404000
406000
408000
410000
412000
6386000
6384000
6382000
6380000
6378000

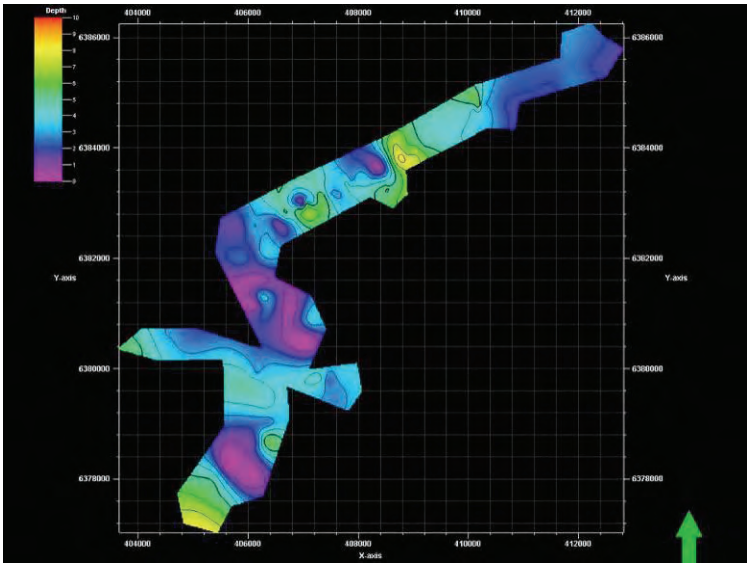
Depth
X-axis
Y-axis
404000
406000
408000
410000
412000
6386000
6384000
6382000
6380000
6378000

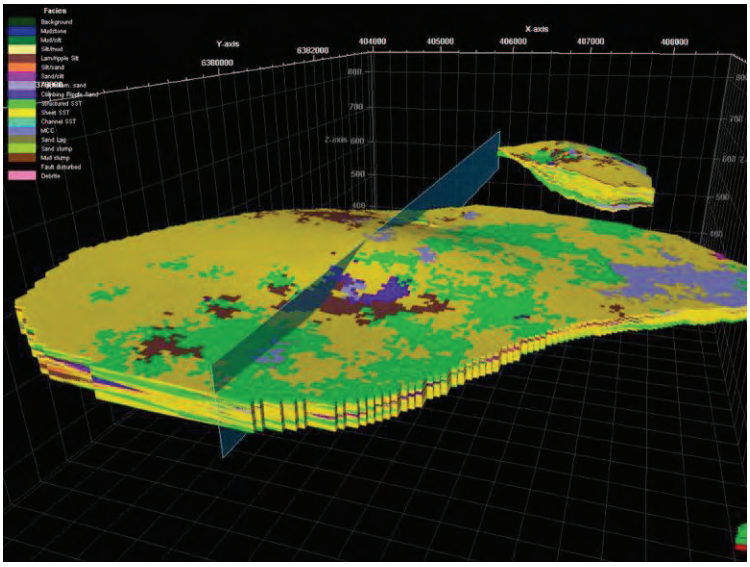
Facies
Background
Mudstone
Mudsilt
Silt/mud
Lam/ripple Slt
Silt/sand
Sand/slt
Ripple/lam. sand
Climbing Ripple Sand
Structured SST
Sheet SST
Channel SST
MCC
Sand Lag
Sand slump
Mud slump
Fault disturbed
Debrite
Y-axis
6380000
6382000
X-axis
404000
405000
406000
407000
408000
Z-axis
800
700
600
500
400

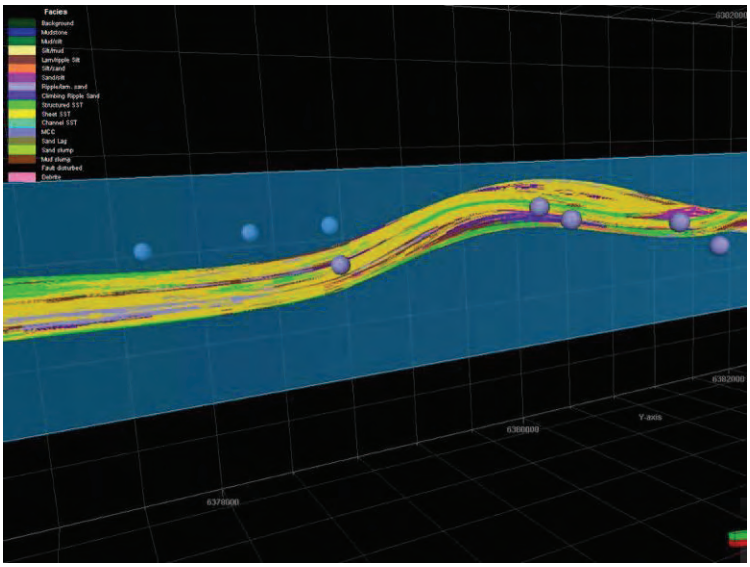
Facies
Background
Mudstone
Mudsilt
Silt/mud
Lam/ripple Slt
Silt/sand
Sand/slt
Ripple/lam. sand
Climbing Ripple Sand
Structured SST
Sheet SST
Channel SST
MCC
Sand Lag
Sand slump
Mud slump
Fault disturbed
Debrite
6382000
Y-axis
6380000
6378000

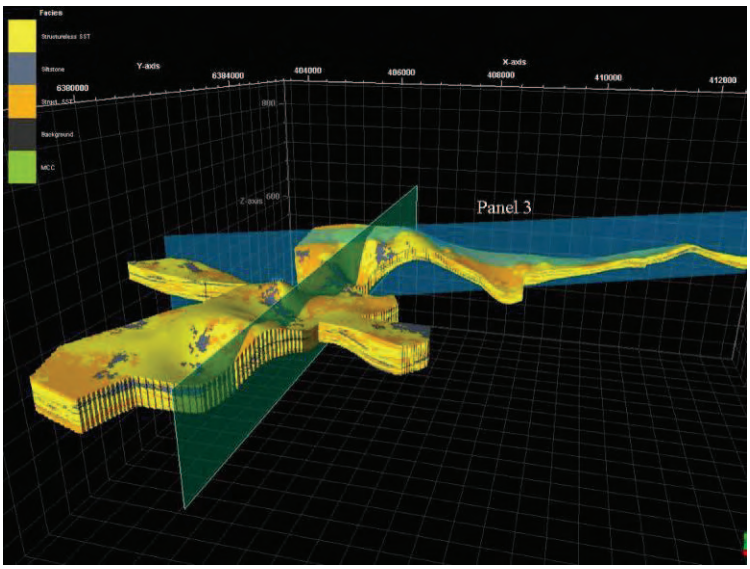
Facies
Structureless SST
Siltstone
6380000
Background
MCC
Y-axis
6384000
404000
406000
X-axis
408000
410000
412000
800
Z-axis
600
Panel 3

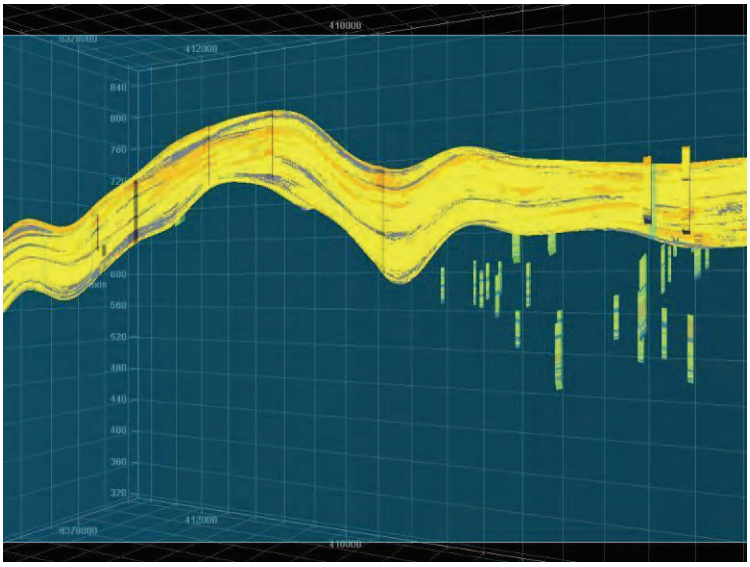

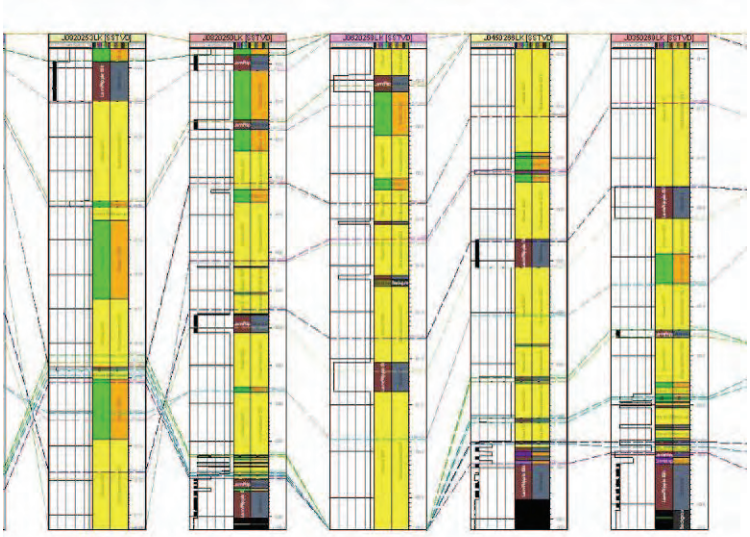

Current work

- Project hand-in: 1 September 2008
- Finishing Write-up

Appendix C

Petrel Thickness Maps

Petrel Thickness Maps

The images herein represent all the thickness maps created during experimentation with various methods in Petrel.

The first 10 images were created during the early stages. Five different border polygons were used, separated by several hundred metres from the data points. In this case, thickness maps could be produced for only the sandstone prone lobes and lobe-elements, as their pinch-out patterns made it impossible to accurately represent the siltstones separating them. Also, these thickness maps were created using the “Create Thickness Map” function within Petrel, and the resulting colour patterns and scales were left unchanged.

The second set of thickness maps represents the last run. Here all 19 maps, namely the sandstone prone lobes and lobe-elements, as well as their separating thin-bedded intervals, could be produced. The reason for this is discussed in Chapters 6 and 7. For these maps a much tighter border polygon was used, making it possible to more accurately extrapolate the data in 3D. These thickness maps were created using the “Arithmetic” function in Petrel, the thicknesses given by $Z = Z^{Top} – Z^{Bottom}$. The colour pattern was left unchanged, but the vertical thickness scale was adjusted for each map. Most of them used a fixed vertical scale to better compare them. This scale for sandstone prone lobes and lobe-elements had to be reduced for lower stratigraphic units, as their drastic decrease in thickness meant they were no longer comparable to the upper units. The sandstone isopach maps also show the inferred axial zones and lobe fringes.

Both sets of thickness maps are presented from the top (namely Lobe 6) downward.

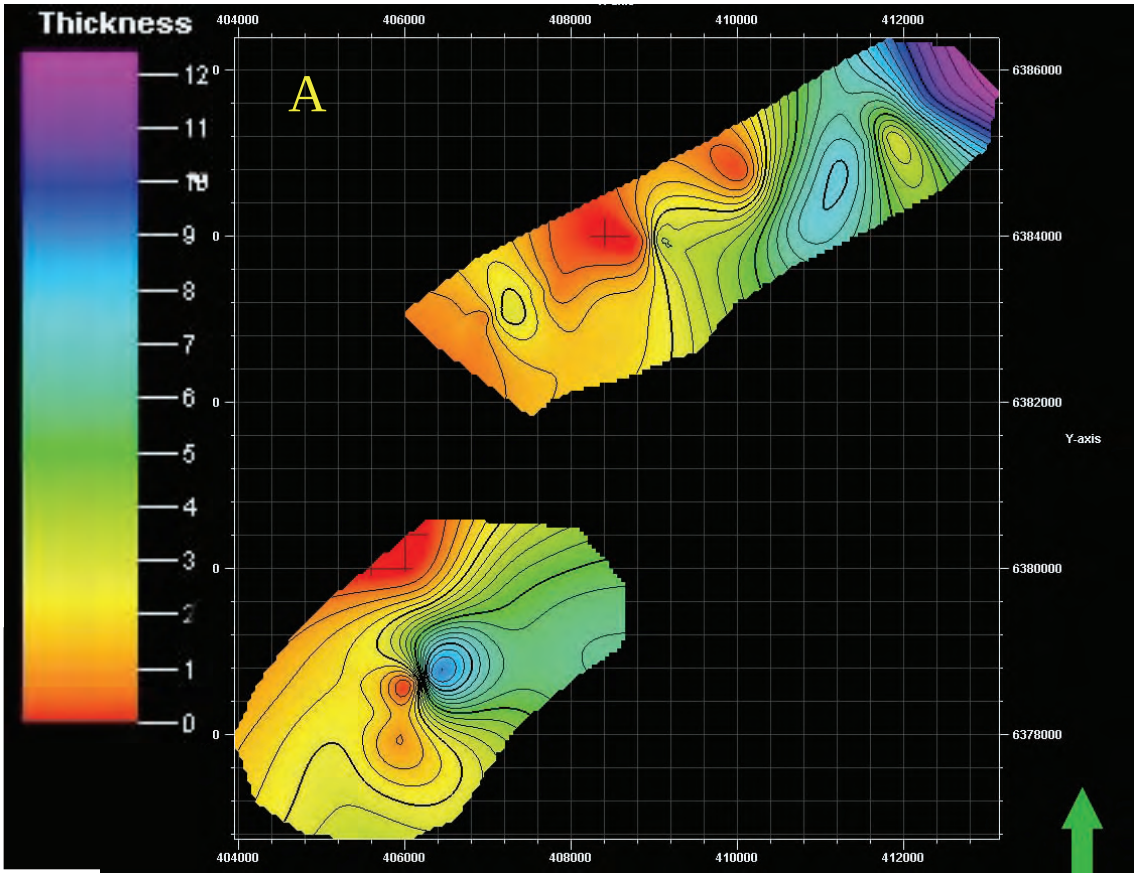
Thickness
12
11
9
8
7
6
5
4
3
1
0
A
404000
406000
408000
410000
412000
6386000
6384000
6382000
6380000
6378000
Y-axis

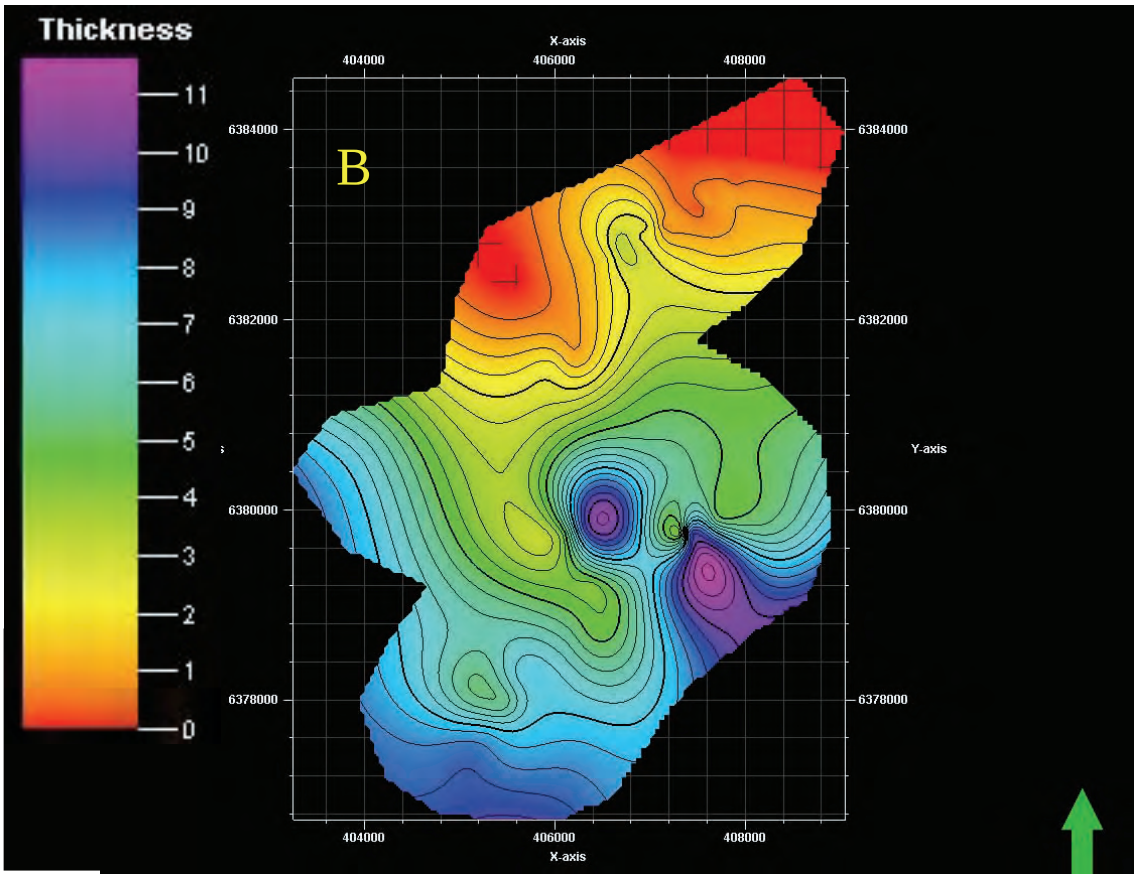
Thickness
11
10
9
8
7
6
5
4
3
2
1
0
B
X-axis
404000
406000
408000
6384000
6382000
6380000
6378000
Y-axis

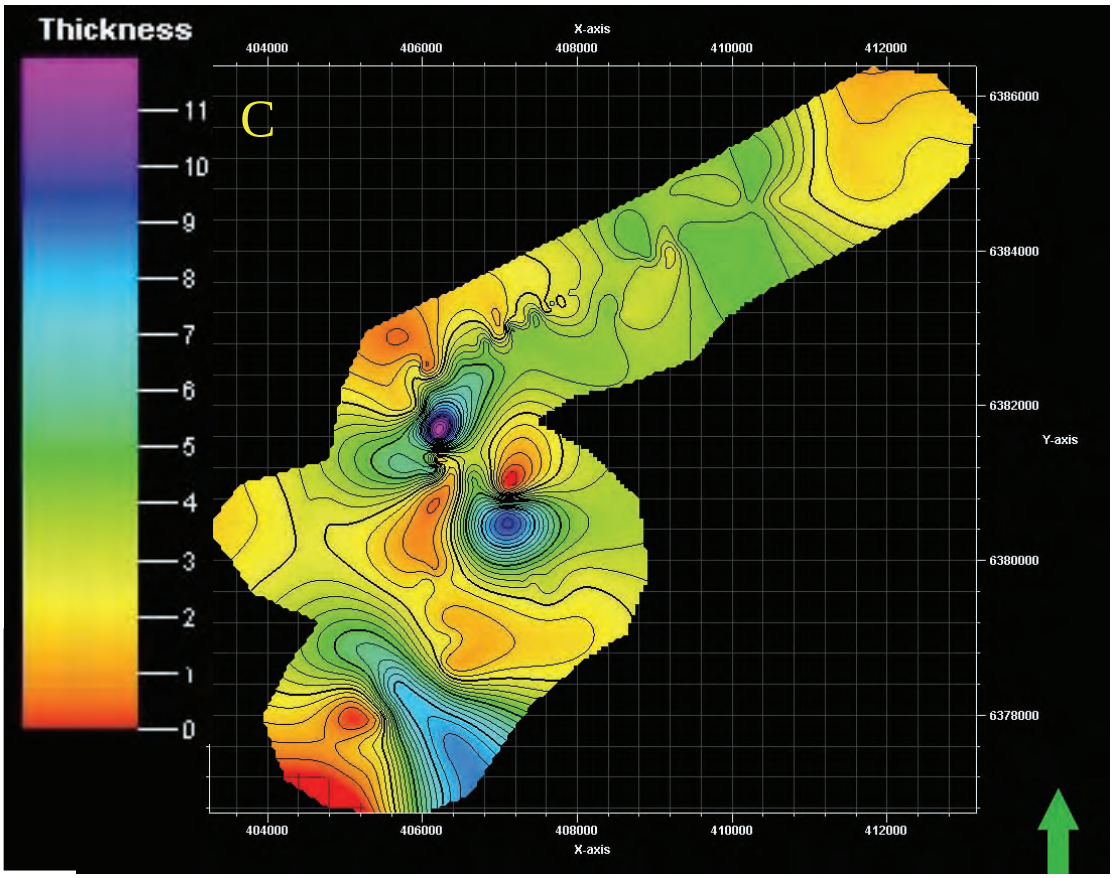
Thickness
C
X-axis
404000
406000
408000
410000
412000
Y-axis
6386000
6384000
6382000
6380000
6378000
11
10
9
8
7
6
5
4
3
2
1
0

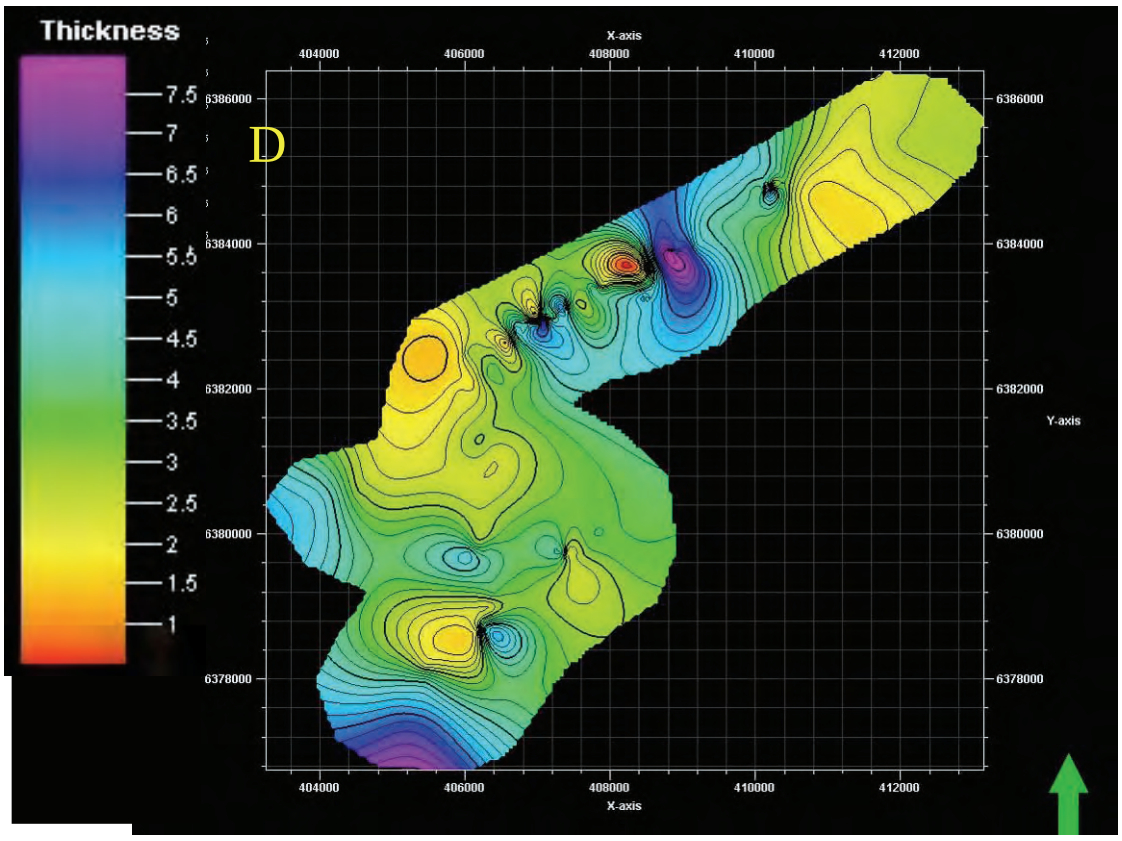
Thickness
D
X-axis
404000
406000
408000
410000
412000
Y-axis
6386000
6384000
6382000
6380000
6378000
7.5
7
6.5
6
5.5
5
4.5
4
3.5
3
2.5
2
1.5
1

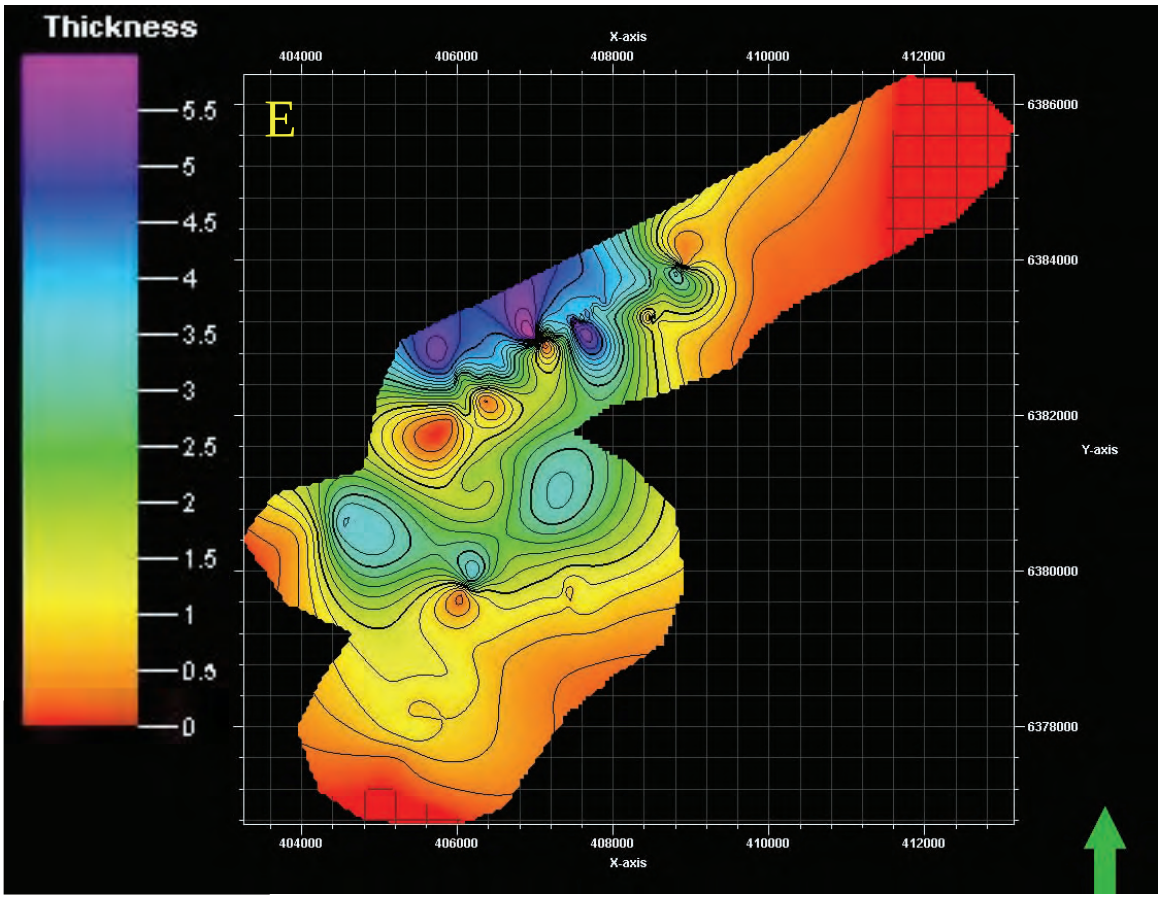
Thickness
X-axis
404000
406000
408000
410000
412000
E
6386000
6384000
6382000
Y-axis
6380000
6378000
5.5
5
4.5
4
3.5
3
2.5
2
1.5
1
0.5
0

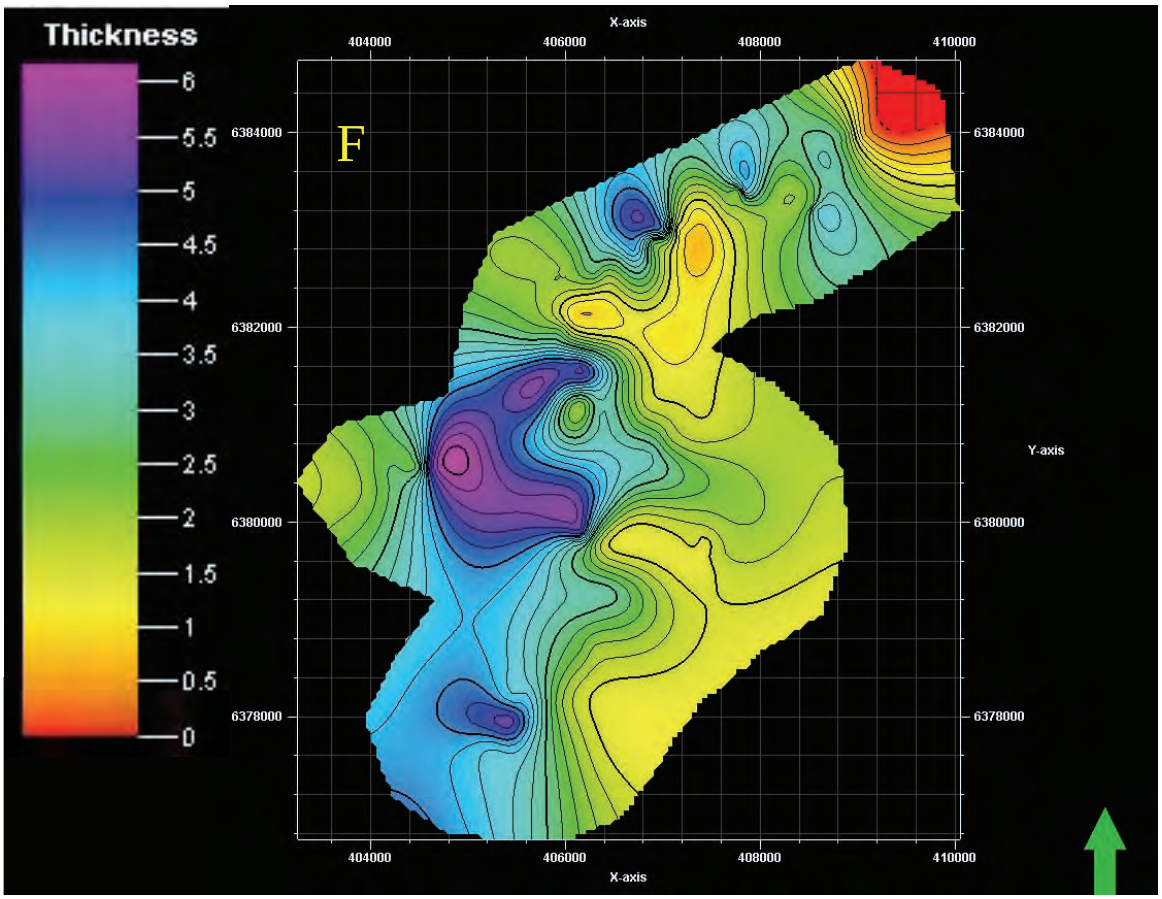
Thickness
X-axis
404000
406000
408000
410000
F
6384000
6382000
Y-axis
6380000
6378000
6
5.5
5
4.5
4
3.5
3
2.5
2
1.5
1
0.5
0

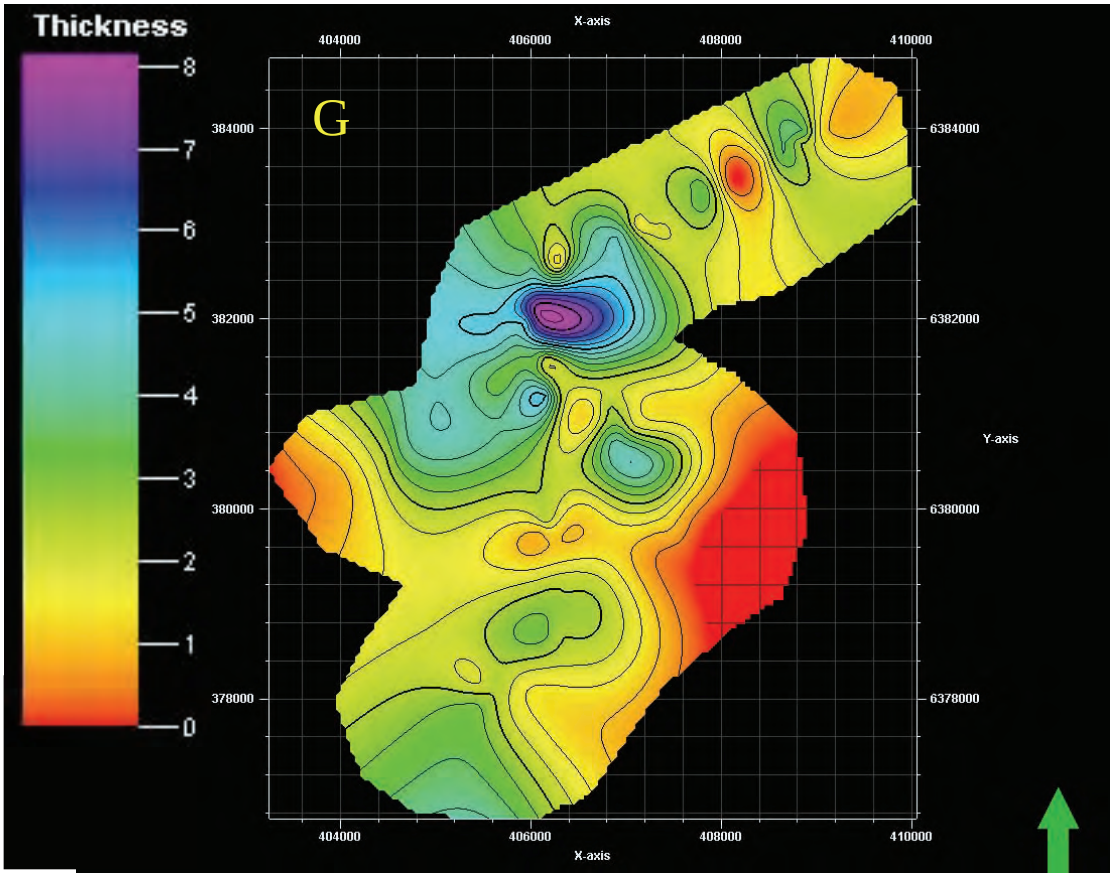
Thickness
8
7
6
5
4
3
2
1
0
X-axis
404000
406000
408000
410000
384000
382000
380000
378000
6384000
6382000
6380000
6378000
Y-axis
G

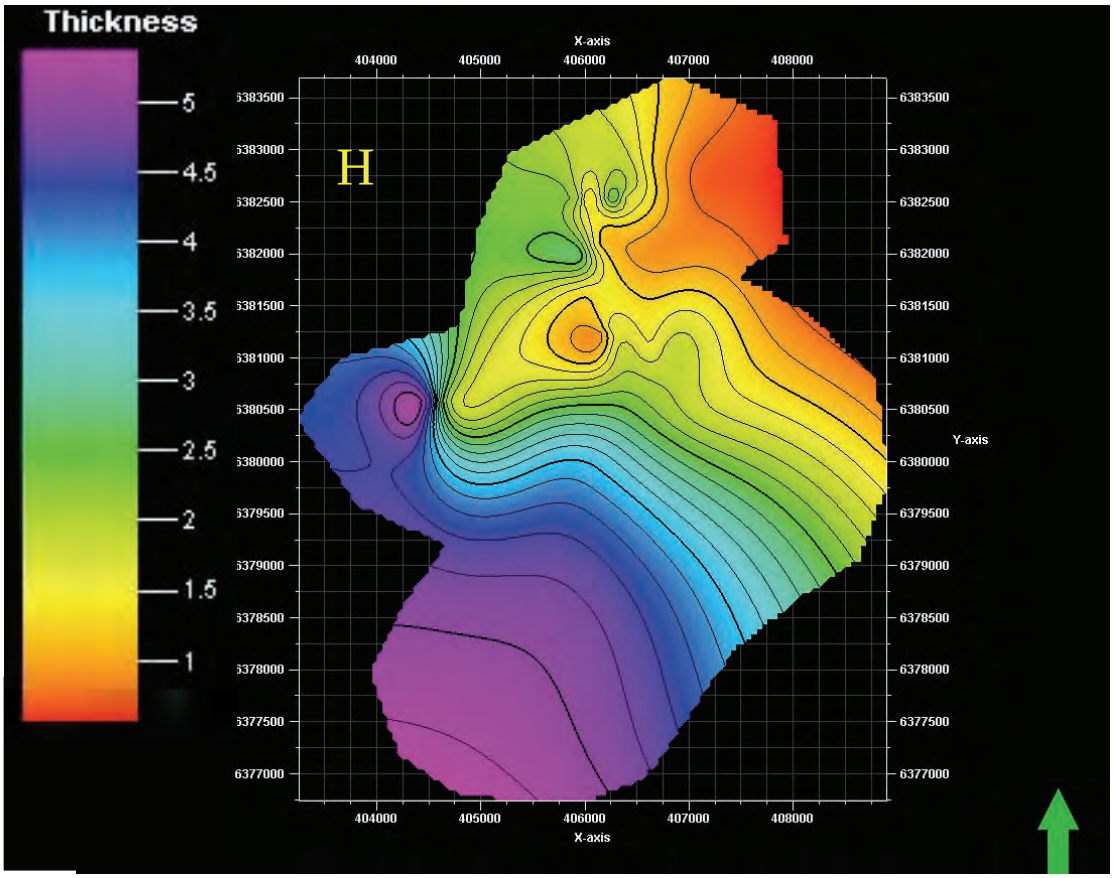
Thickness
5
4.5
4
3.5
3
2.5
2
1.5
1
X-axis
404000
405000
406000
407000
408000
6383500
6383000
6382500
6382000
6381500
6381000
6380500
6380000
6379500
6379000
6378500
6378000
6377500
6377000
Y-axis
H

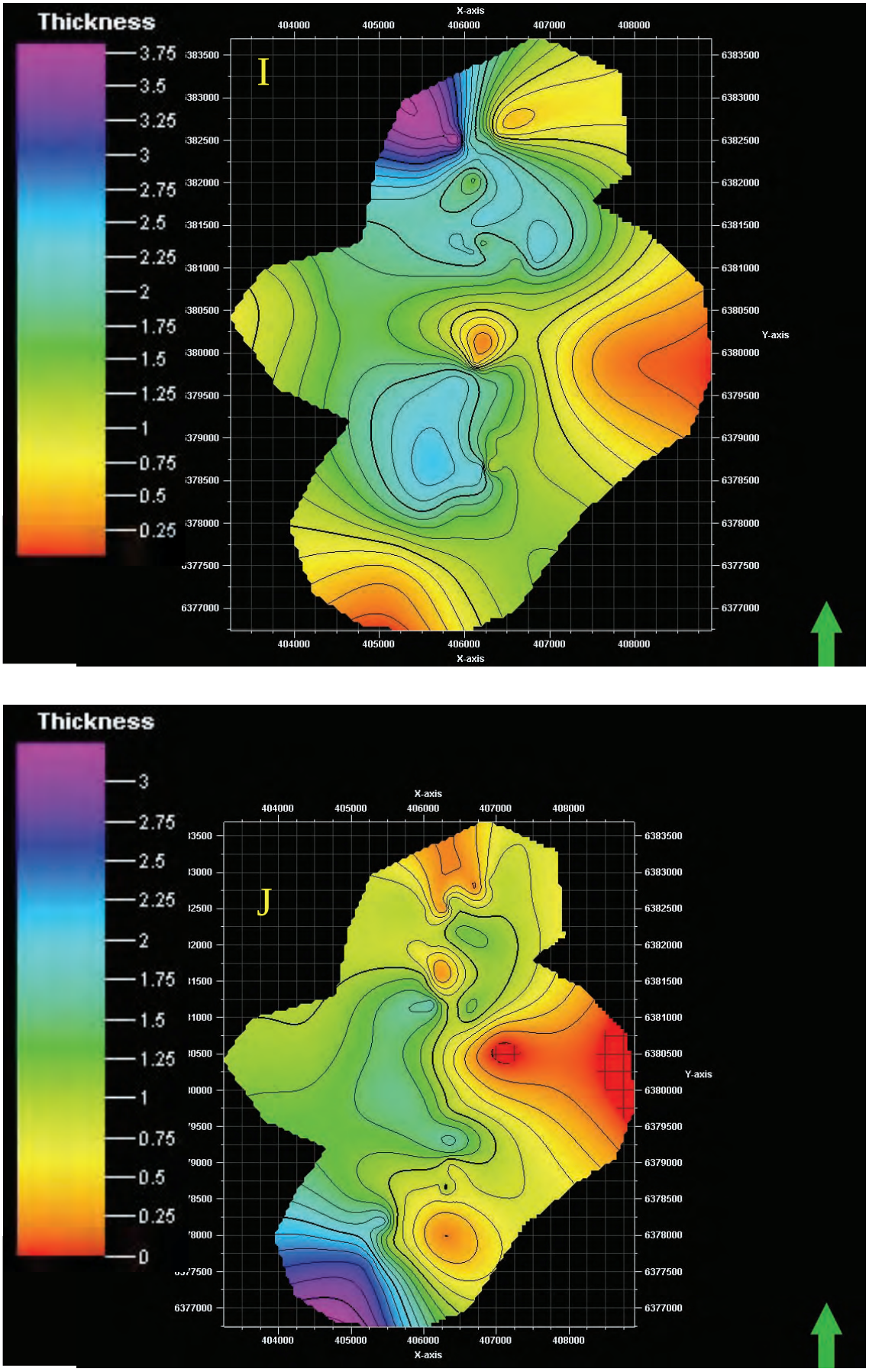

Figure C.1 The first set of Thickness Maps.

Figure |C.1 Legend

A - Lobe 6

B - Upper Lobe 5

C - Lower Lobe 5

D - Upper Lobe 4

E - Lower Lobe 4

F - Upper Lobe 2

G - Lower Lobe 2

H - Lobe 1

I - Sub Lobe 2

J - Sub Lobe 1

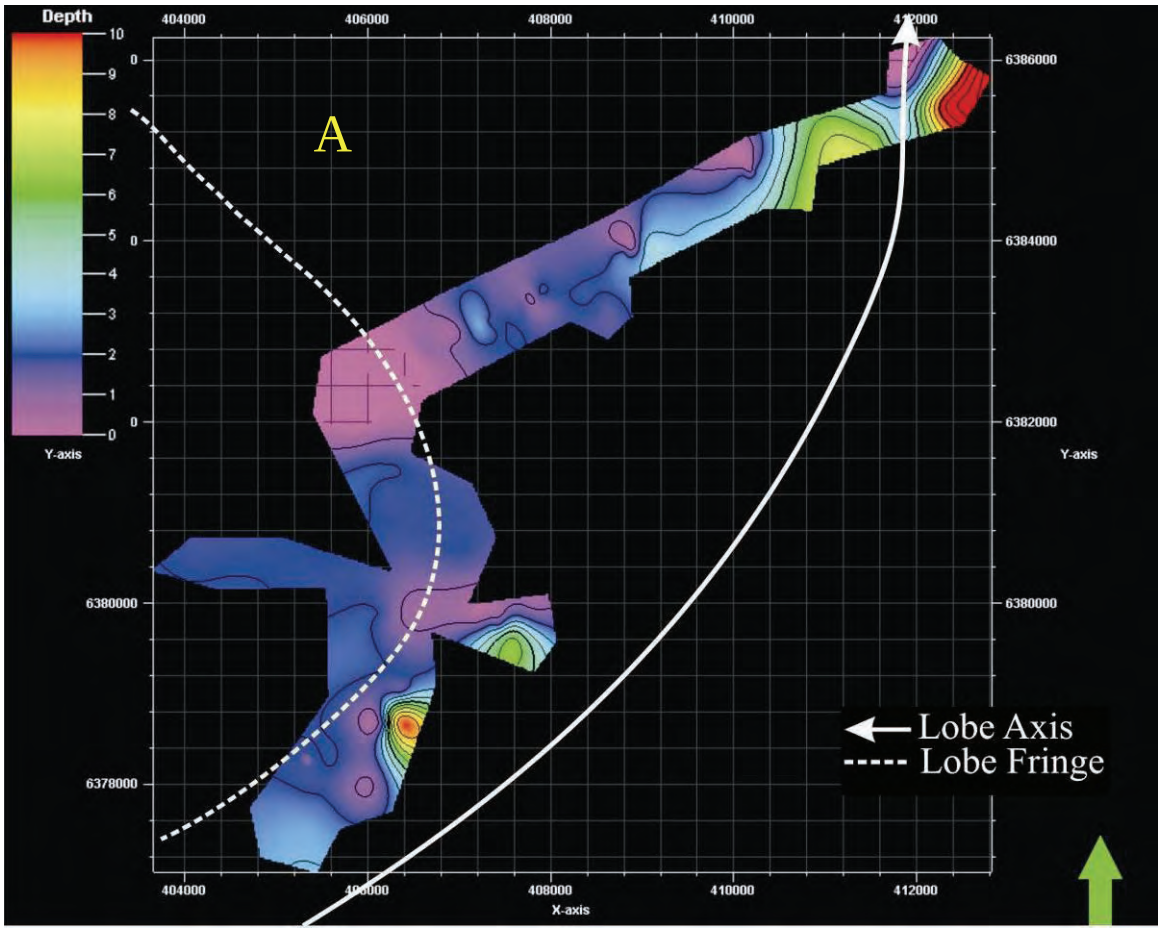
Depth
10
9
8
7
6
5
4
3
2
1
0
Y-axis
A
404000
406000
408000
410000
412000
6386000
6384000
6382000
6380000
6378000
Y-axis
X-axis
Lobe Axis
Lobe Fringe

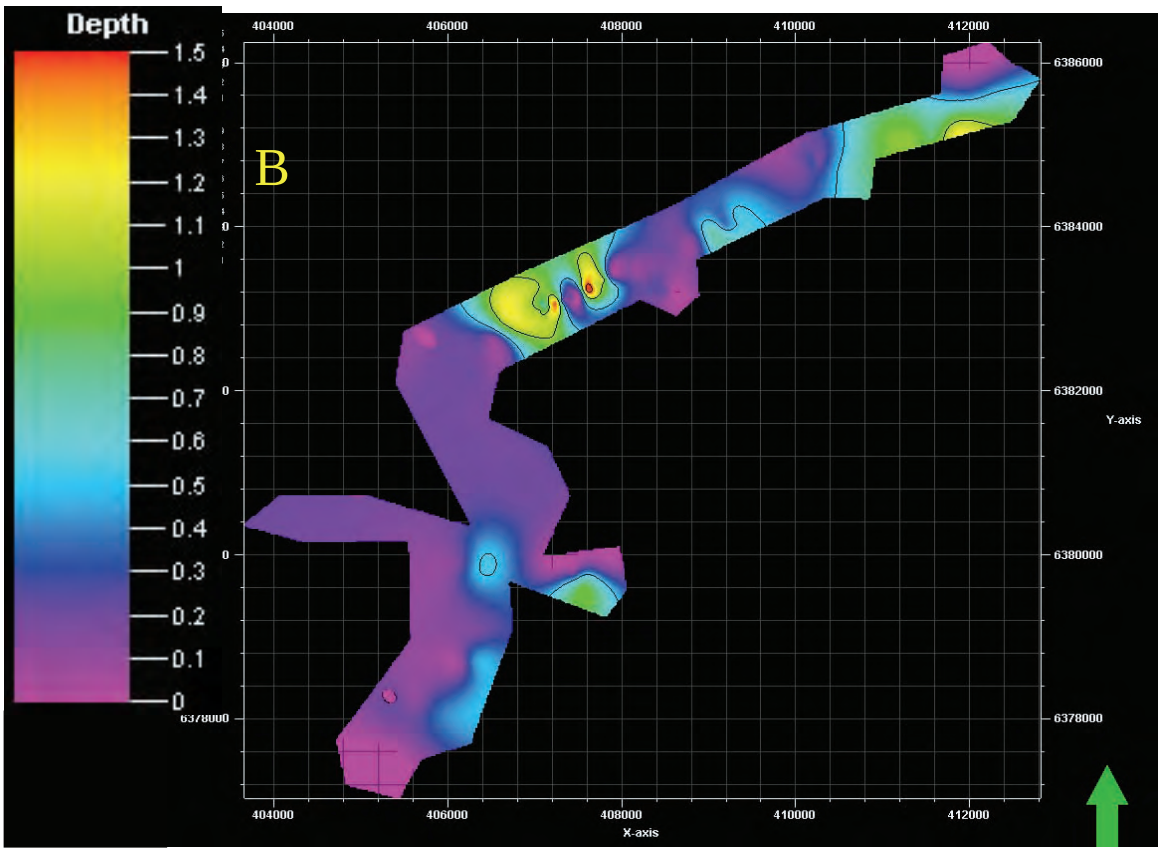
Depth
1.5
1.4
1.3
1.2
1.1
1
0.9
0.8
0.7
0.6
0.5
0.4
0.3
0.2
0.1
0
B
404000
406000
408000
410000
412000
6386000
6384000
6382000
6380000
6378000
Y-axis
X-axis

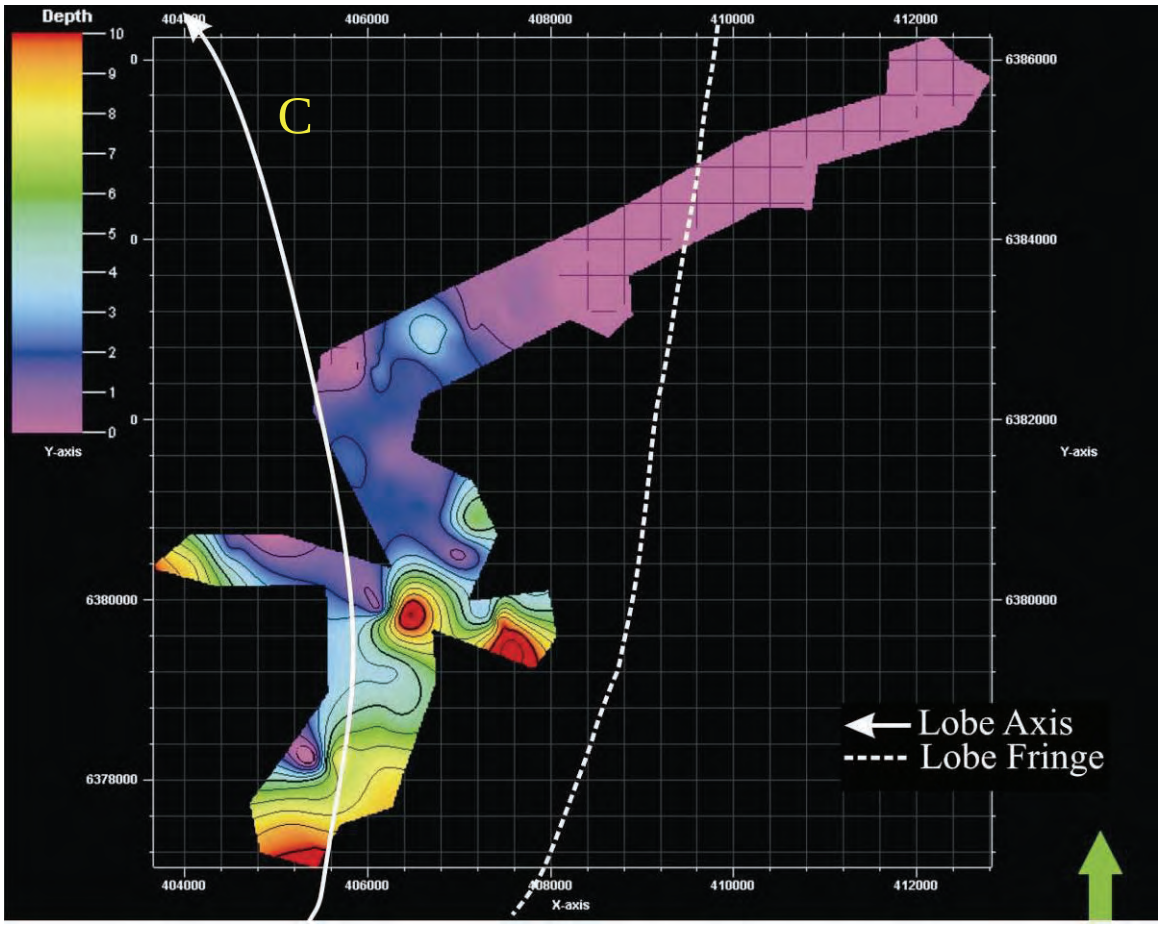
Depth
10
9
8
7
6
5
4
3
2
1
0
Y-axis
C
404000
406000
408000
410000
412000
6386000
6384000
6382000
6380000
6378000
Y-axis
X-axis
Lobe Axis
Lobe Fringe

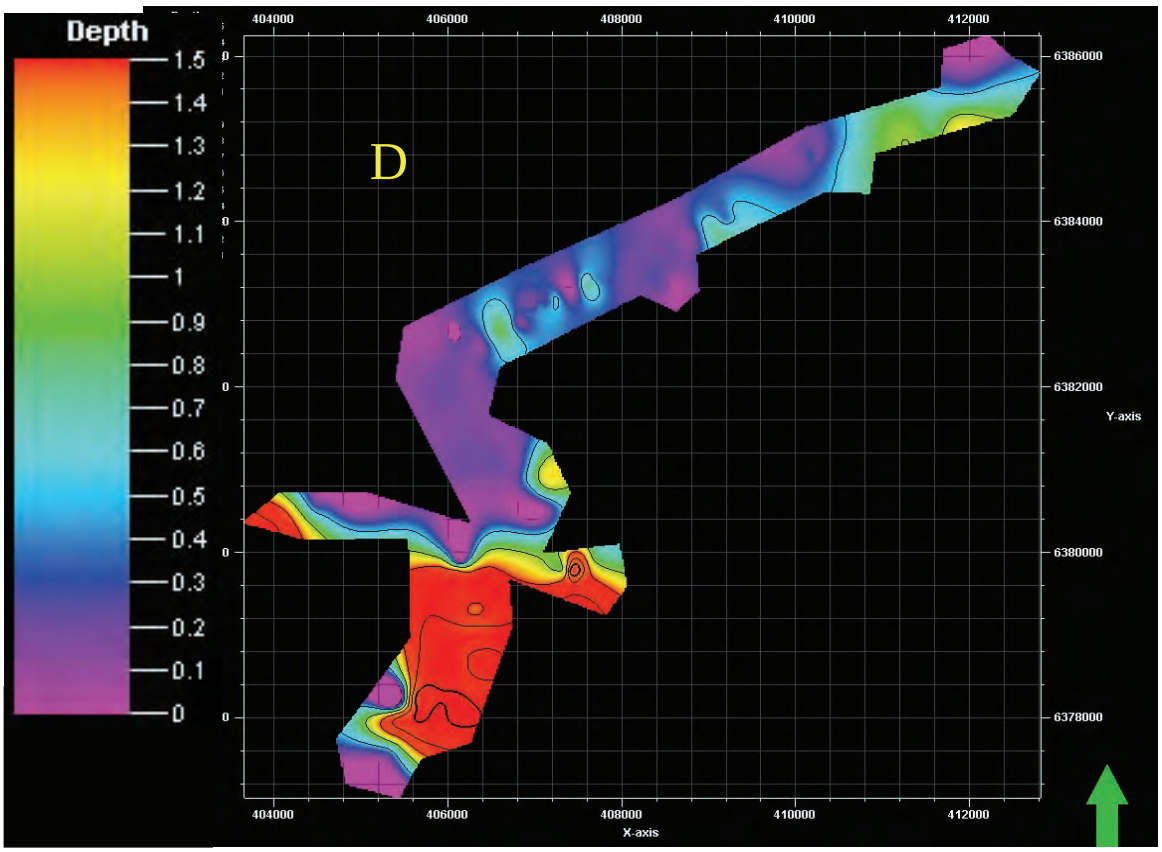
Depth
1.5
1.4
1.3
1.2
1.1
1
0.9
0.8
0.7
0.6
0.5
0.4
0.3
0.2
0.1
0
D
404000
406000
408000
410000
412000
6386000
6384000
6382000
6380000
6378000
Y-axis
X-axis

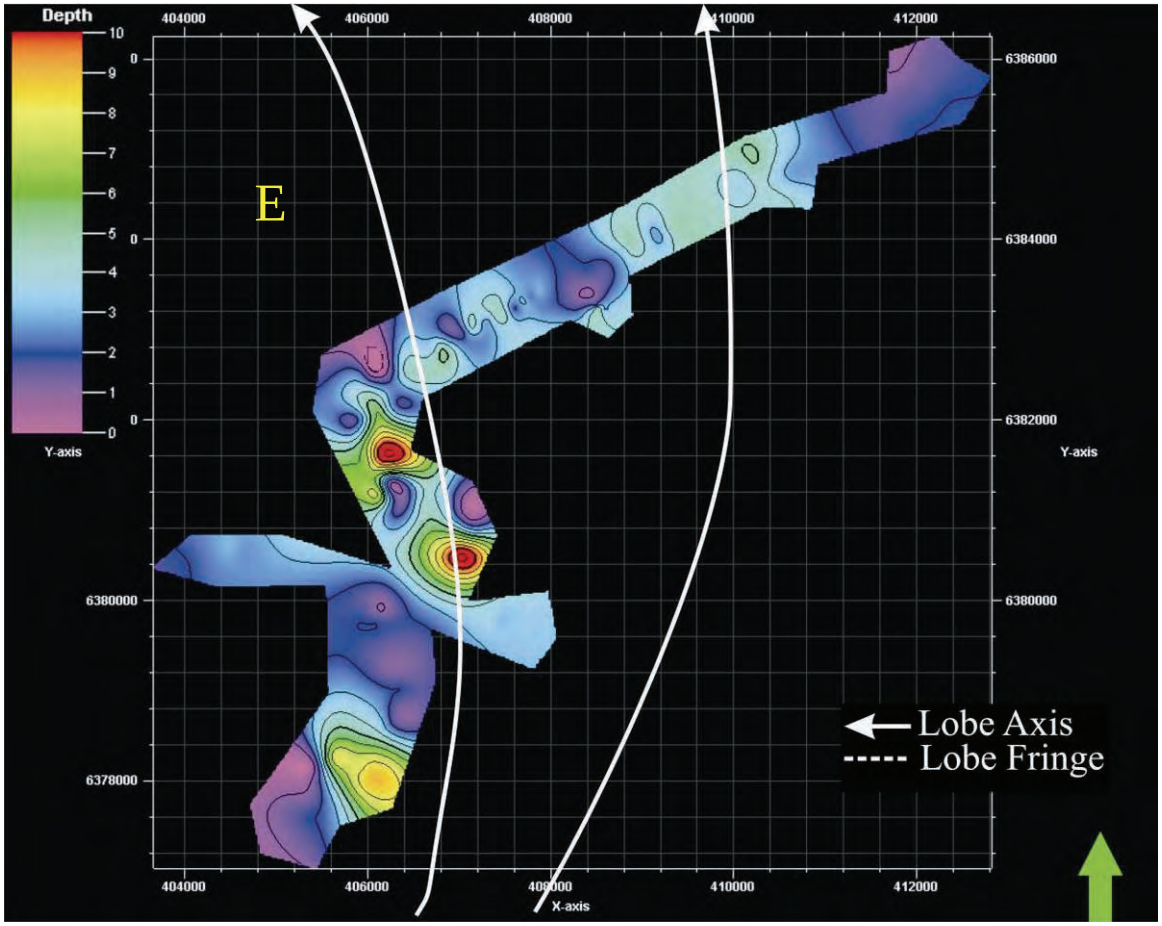
Depth
10
9
8
7
6
5
4
3
2
1
0
Y-axis
E
404000
406000
408000
410000
412000
6386000
6384000
6382000
6380000
6378000
Y-axis
X-axis
Lobe Axis
Lobe Fringe

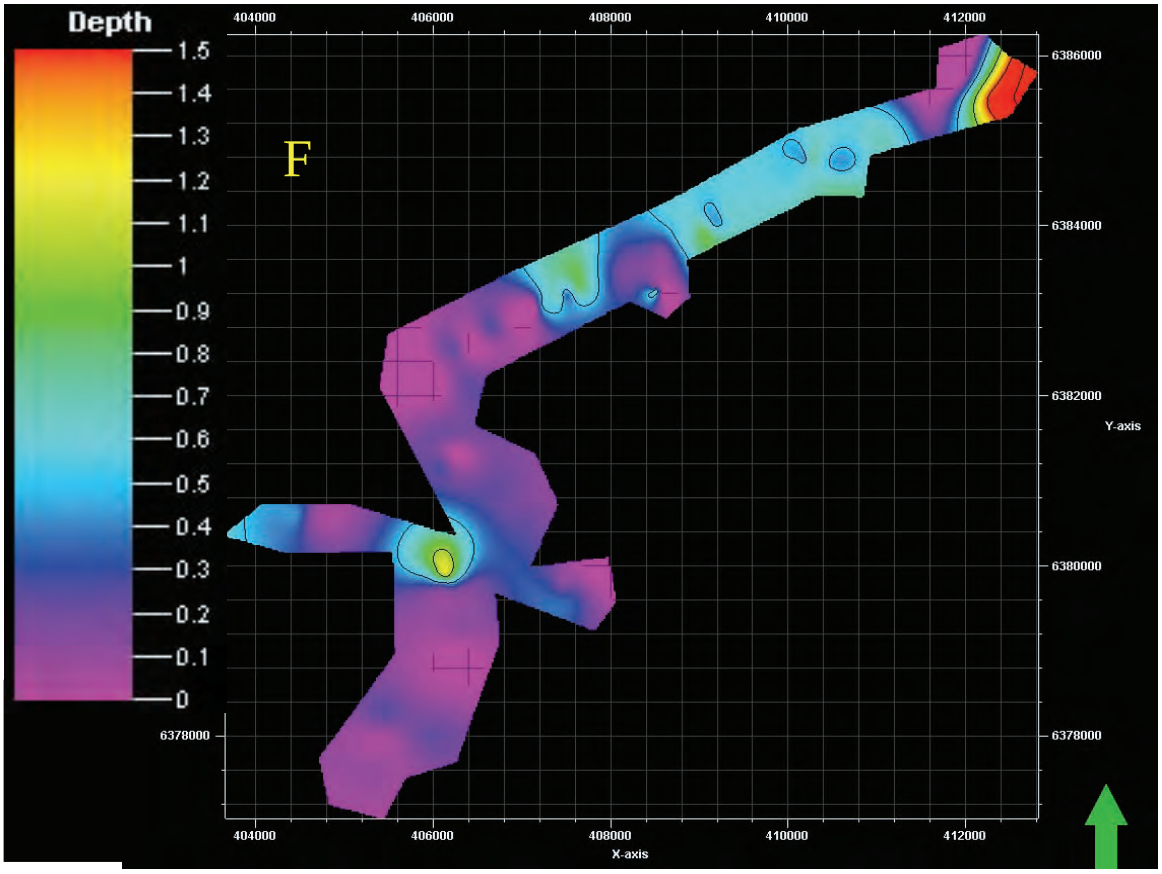
Depth
1.5
1.4
1.3
1.2
1.1
1
0.9
0.8
0.7
0.6
0.5
0.4
0.3
0.2
0.1
0
F
404000
406000
408000
410000
412000
6386000
6384000
6382000
6380000
6378000
Y-axis
X-axis

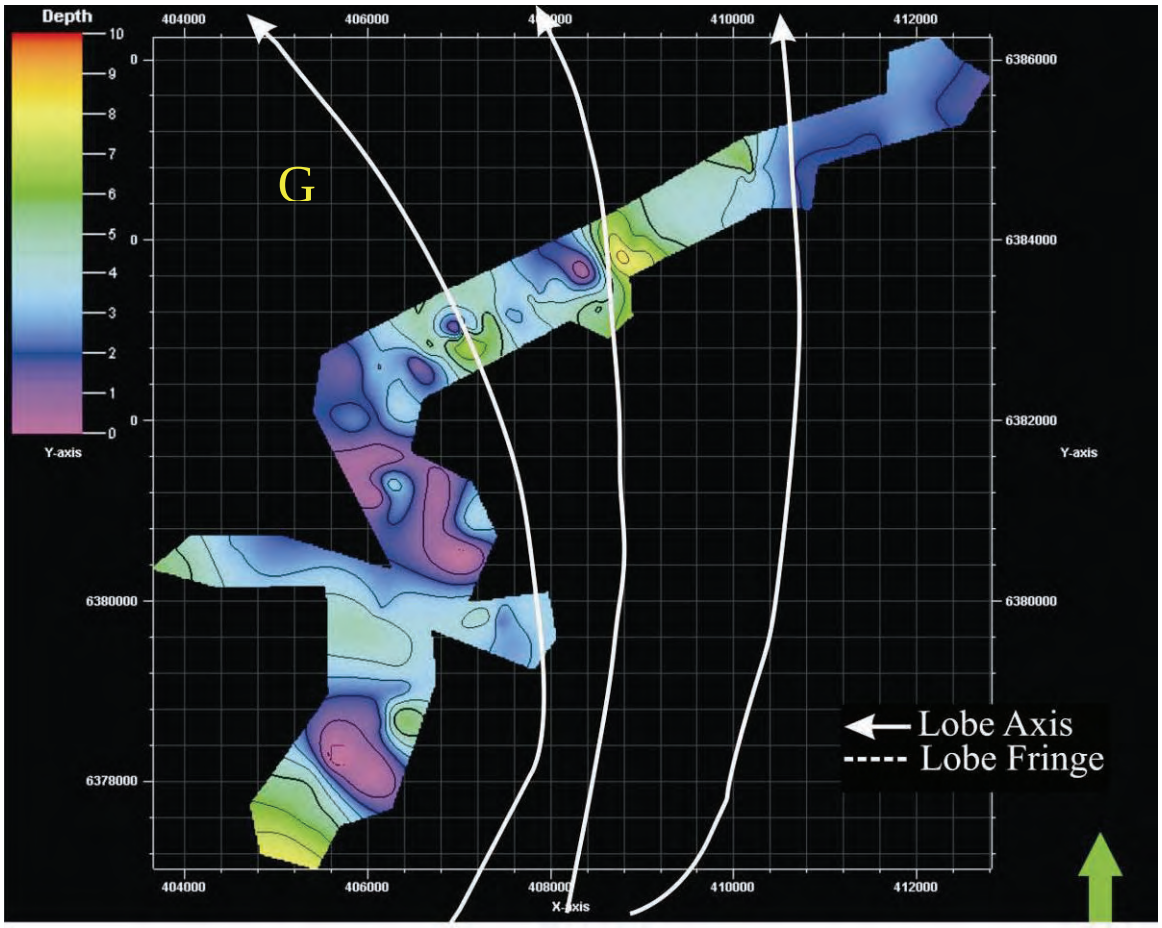
Depth
10
9
8
7
6
5
4
3
2
1
0
Y-axis
404000
406000
410000
412000
6386000
6384000
6382000
Y-axis
6380000
6380000
6378000
G
Lobe Axis
Lobe Fringe
404000
406000
408000
410000
412000
X-axis

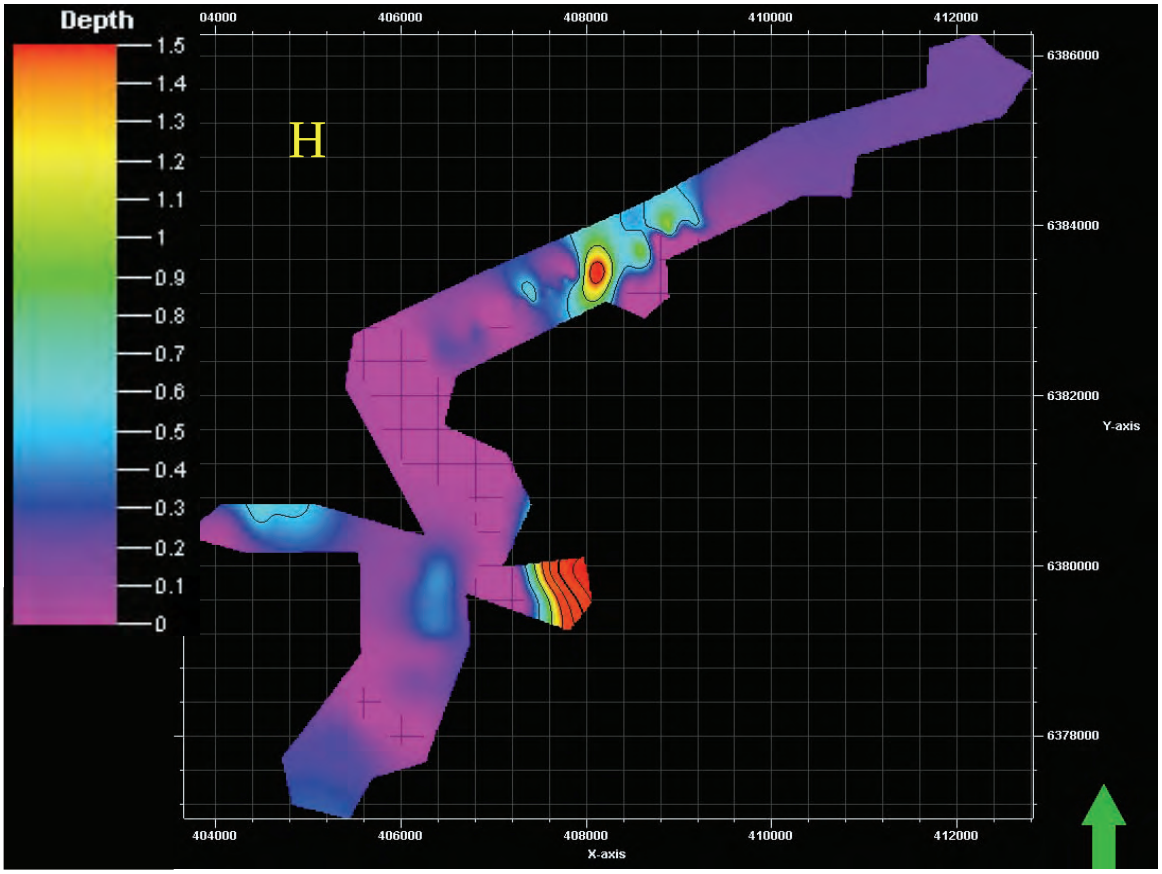
Depth
1.5
1.4
1.3
1.2
1.1
1
0.9
0.8
0.7
0.6
0.5
0.4
0.3
0.2
0.1
0
04000
406000
408000
410000
412000
6386000
6384000
6382000
Y-axis
6380000
6378000
H
404000
406000
408000
410000
412000
X-axis

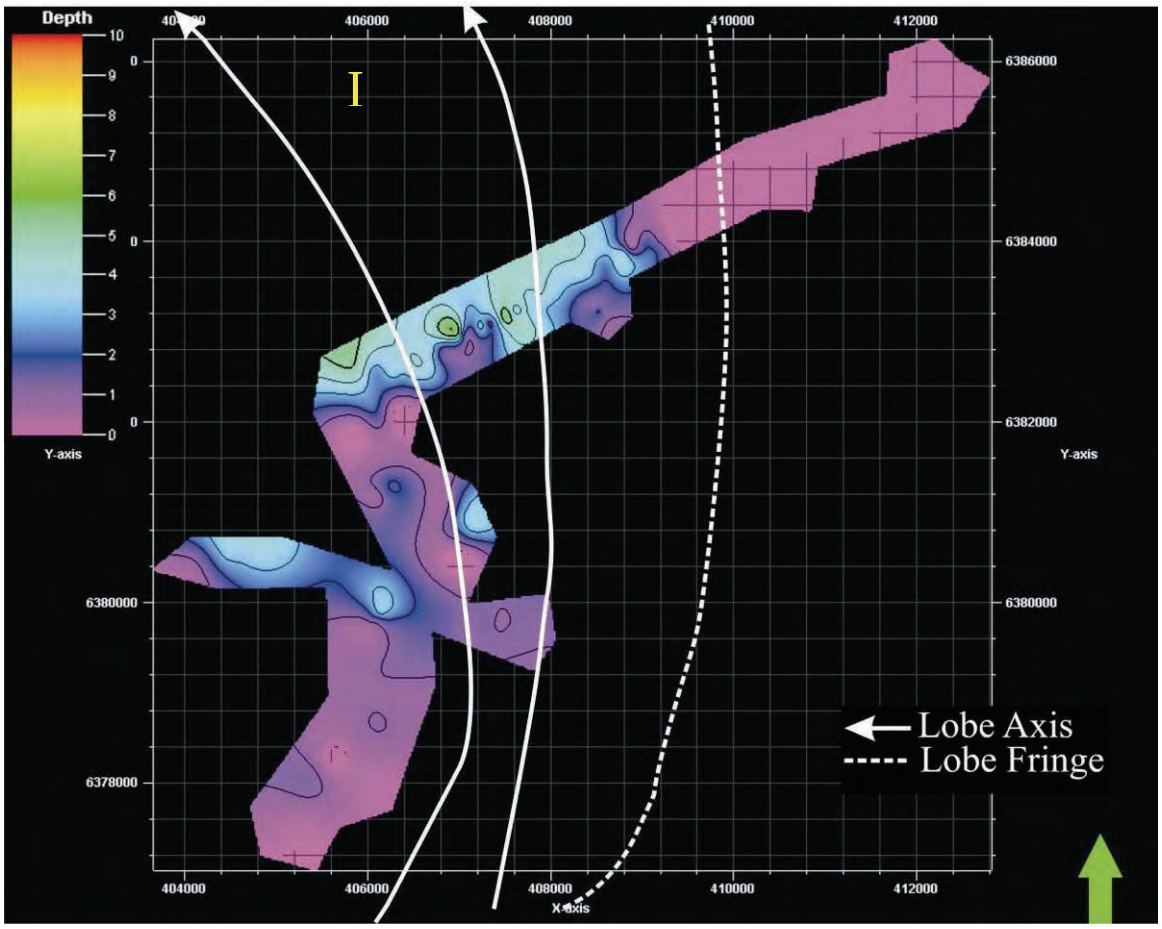
Depth
10
9
8
7
6
5
4
3
2
1
0
Y-axis
I
404000
406000
408000
410000
412000
6386000
6384000
6382000
6380000
6378000
Y-axis
X-axis
Lobe Axis
Lobe Fringe

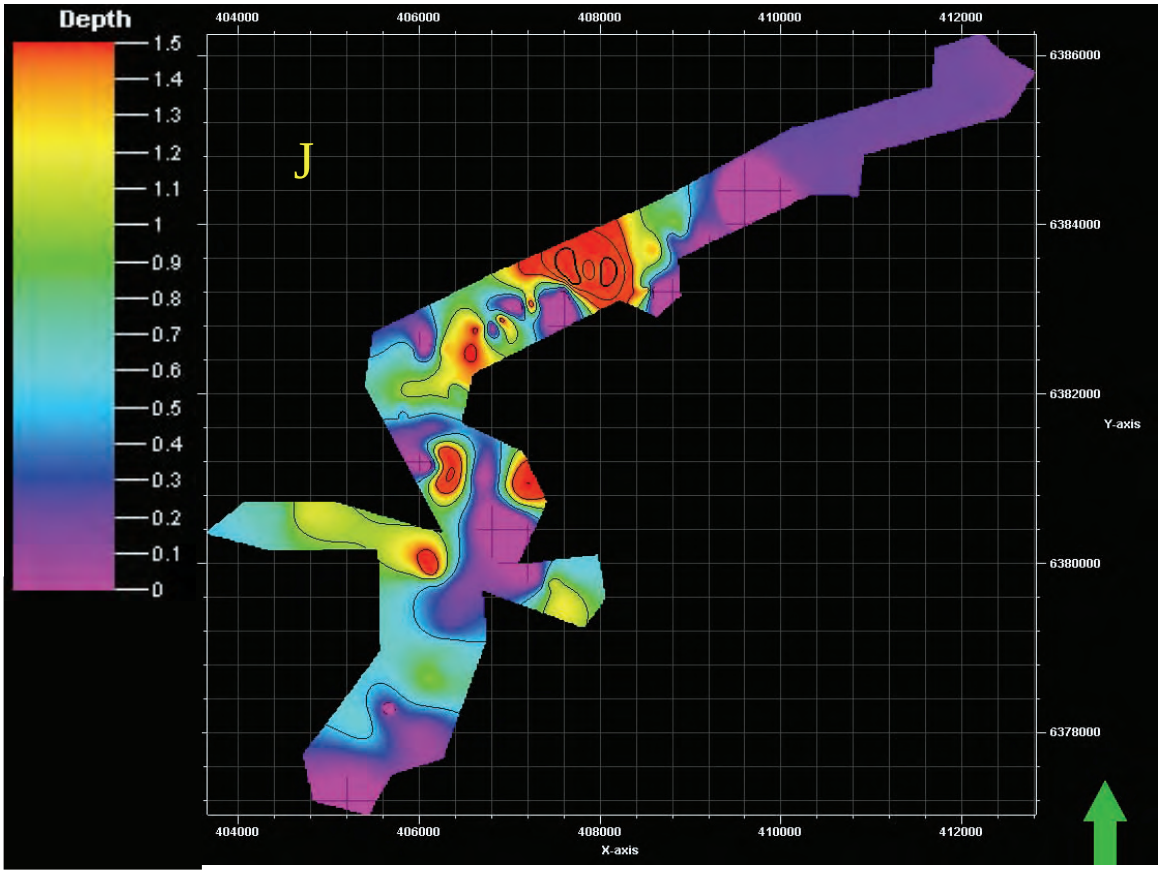
Depth
1.5
1.4
1.3
1.2
1.1
1
0.9
0.8
0.7
0.6
0.5
0.4
0.3
0.2
0.1
0
J
404000
406000
408000
410000
412000
6386000
6384000
6382000
6380000
6378000
Y-axis
X-axis

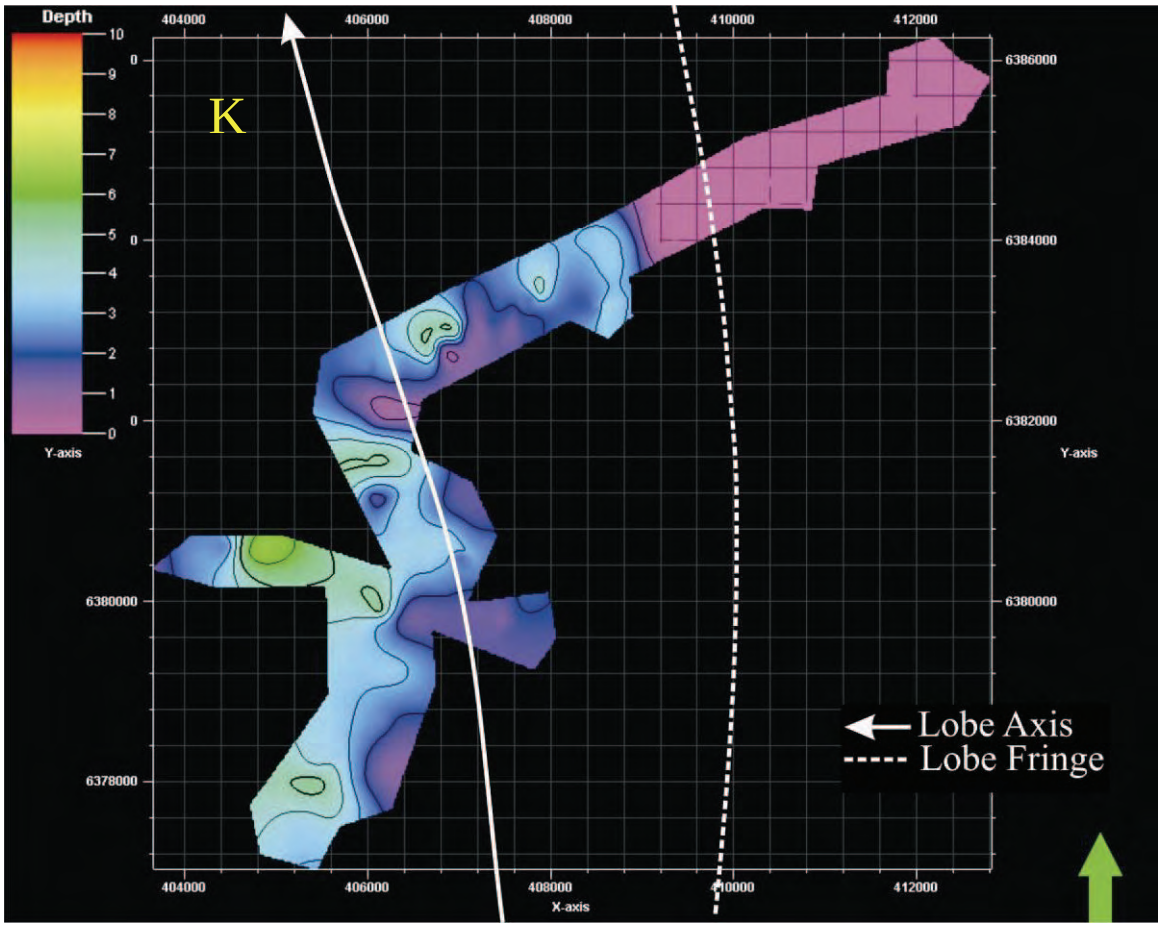
Depth
10
9
8
7
6
5
4
3
2
1
0
Y-axis
K
404000
406000
408000
410000
412000
6386000
6384000
6382000
6380000
6378000
Y-axis
X-axis
Lobe Axis
Lobe Fringe

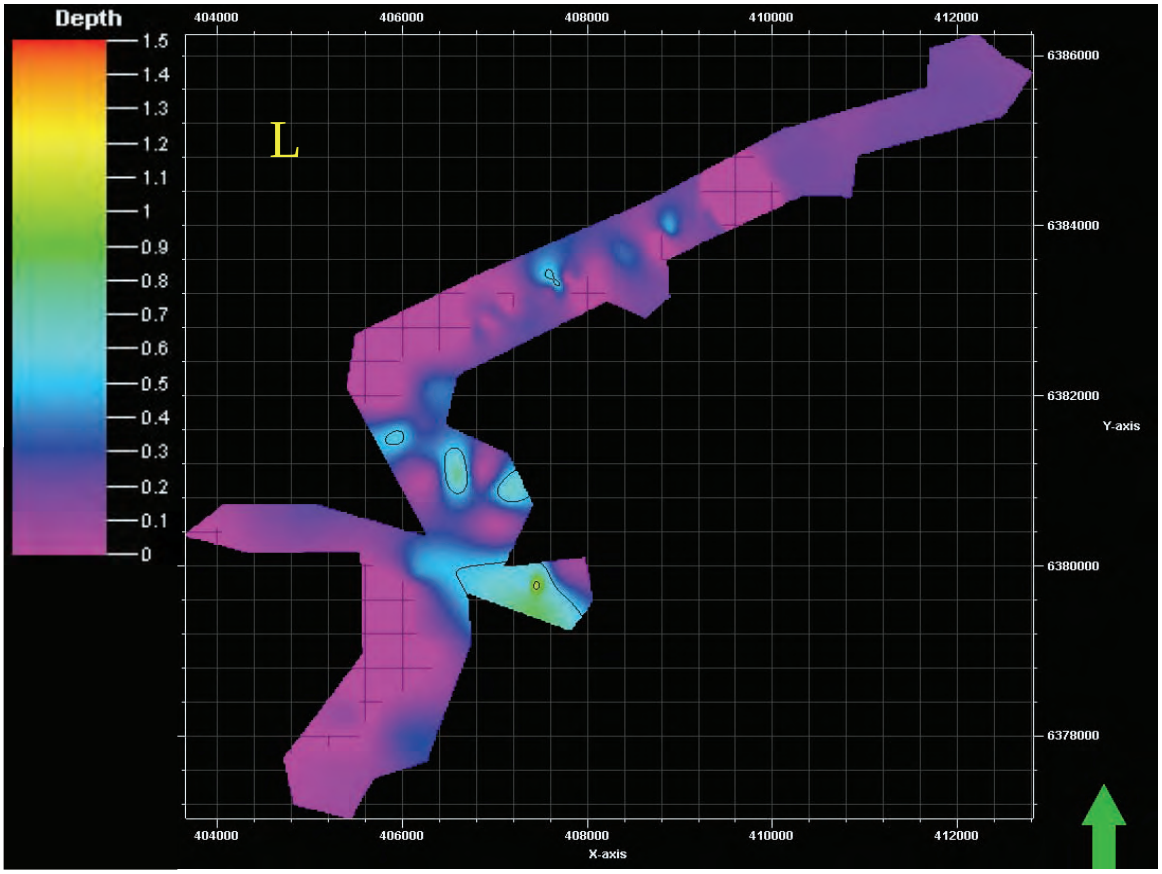
Depth
1.5
1.4
1.3
1.2
1.1
1
0.9
0.8
0.7
0.6
0.5
0.4
0.3
0.2
0.1
0
L
404000
406000
408000
410000
412000
6386000
6384000
6382000
6380000
6378000
Y-axis
X-axis

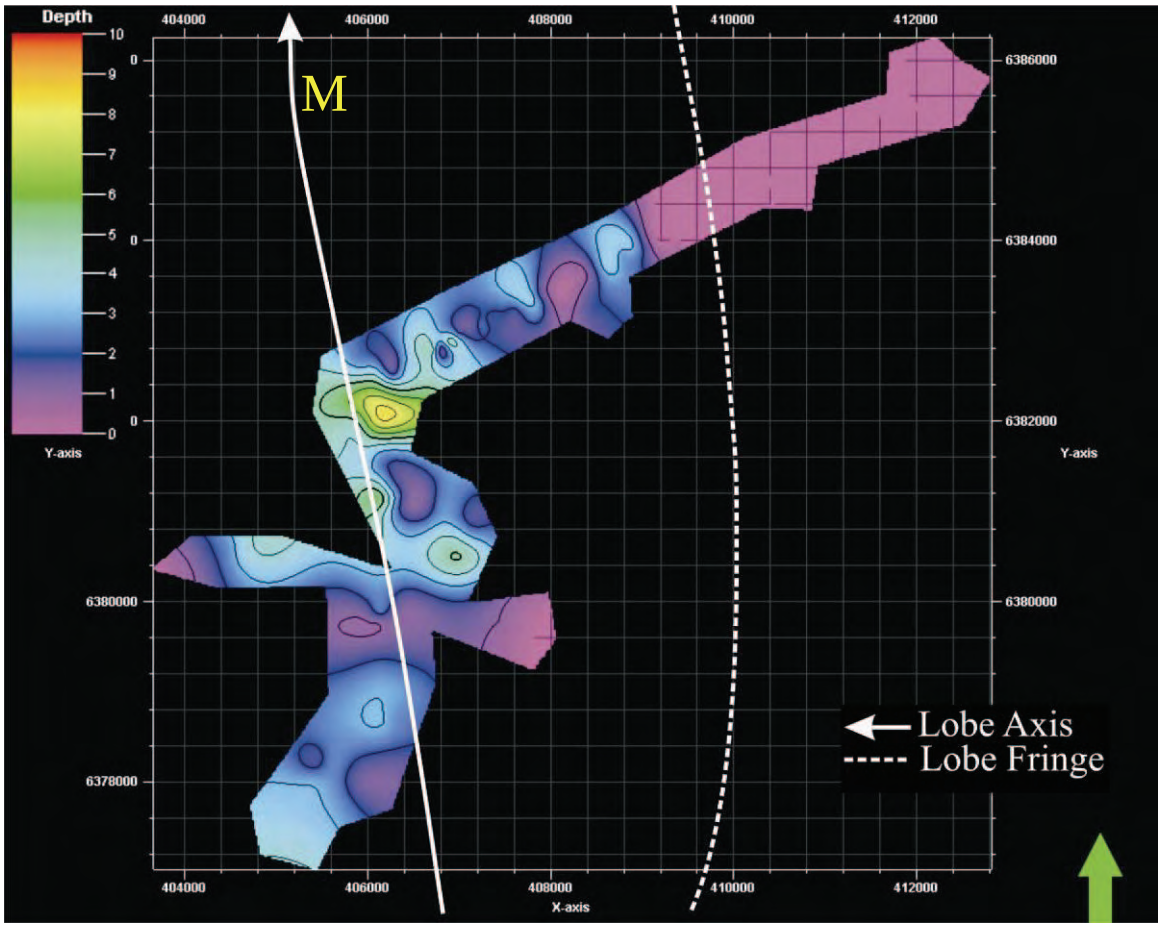
Depth
10
9
8
7
6
5
4
3
2
1
0
Y-axis
404000
406000
408000
410000
412000
X-axis
6386000
6384000
6382000
6380000
6378000
M
Lobe Axis
Lobe Fringe

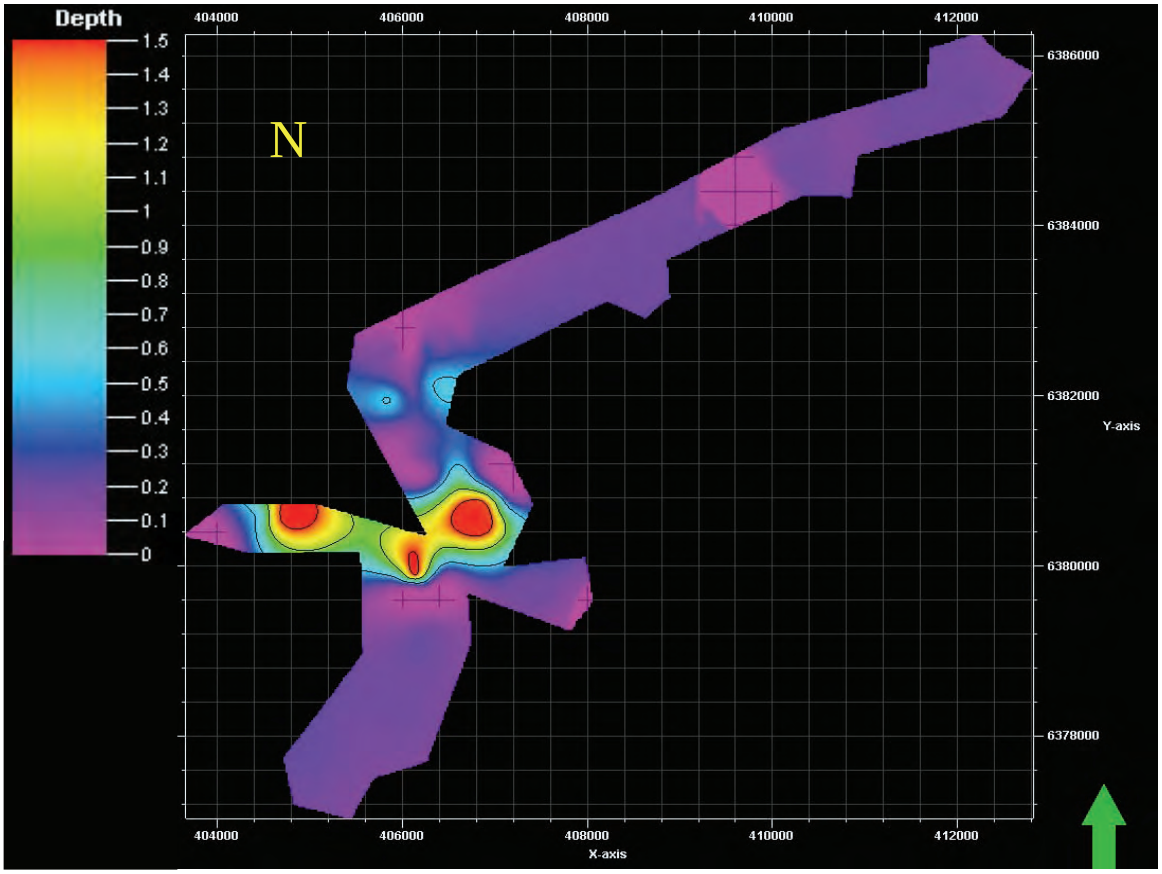
Depth
1.5
1.4
1.3
1.2
1.1
1
0.9
0.8
0.7
0.6
0.5
0.4
0.3
0.2
0.1
0
404000
406000
408000
410000
412000
X-axis
6386000
6384000
6382000
6380000
6378000
Y-axis
N

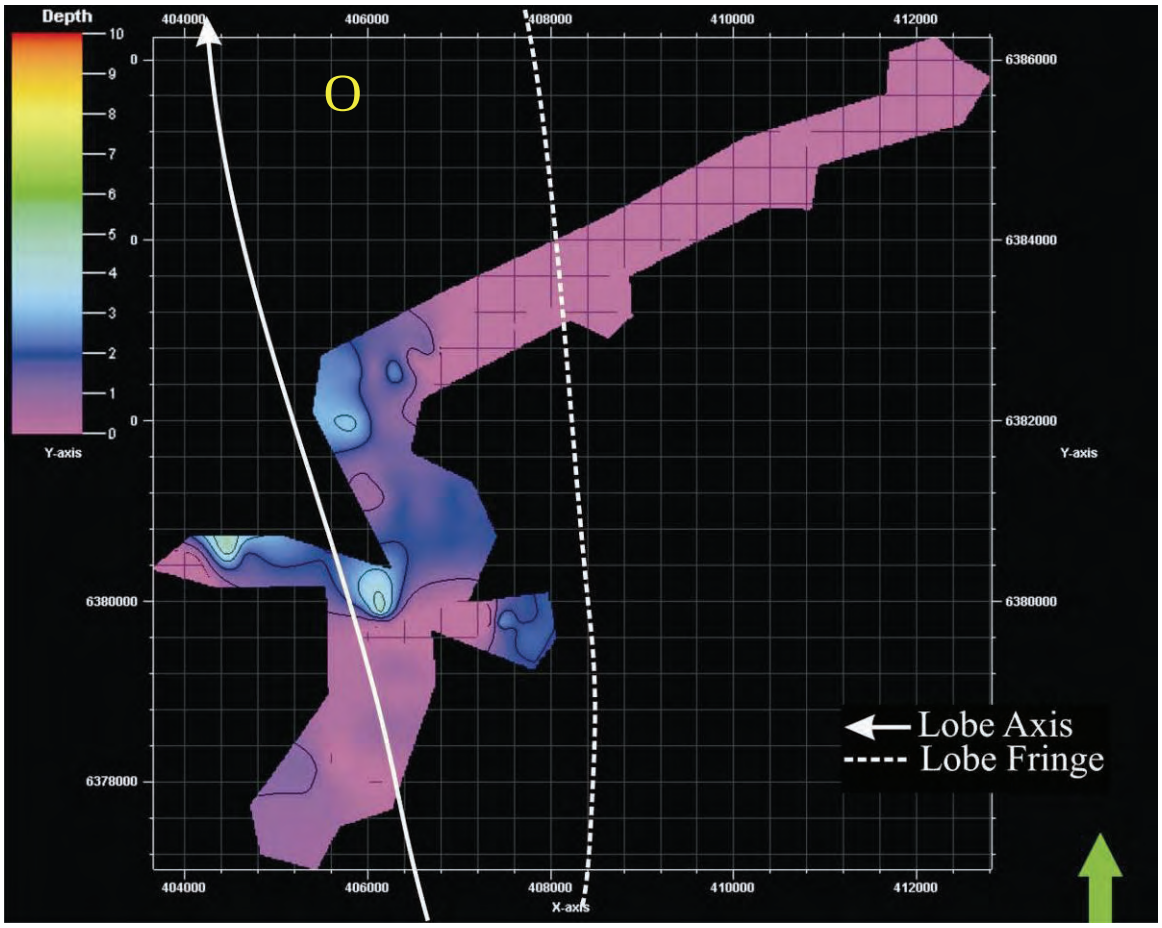
Depth
10
9
8
7
6
5
4
3
2
1
0
Y-axis
O
404000
406000
408000
410000
412000
6386000
6384000
6382000
6380000
6378000
Y-axis
X-axis
Lobe Axis
Lobe Fringe

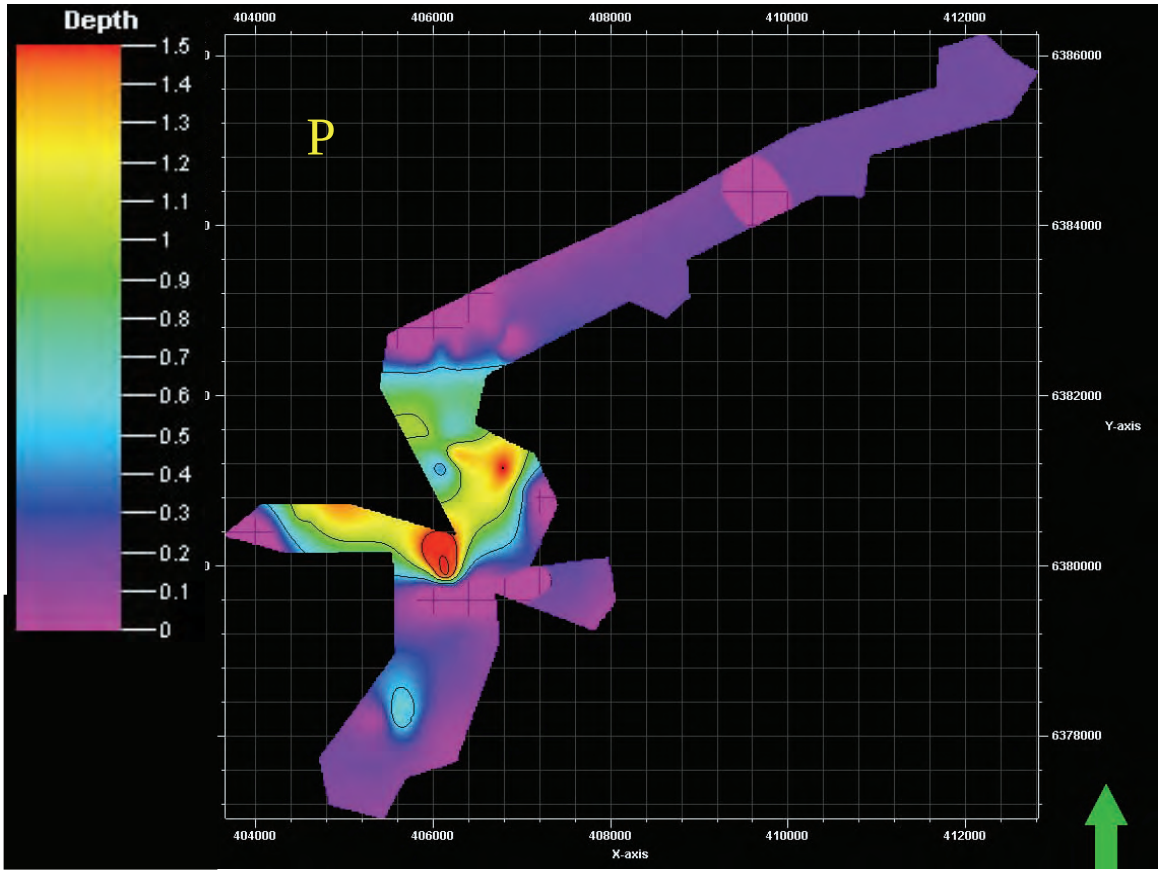
Depth
1.5
1.4
1.3
1.2
1.1
1
0.9
0.8
0.7
0.6
0.5
0.4
0.3
0.2
0.1
0
P
404000
406000
408000
410000
412000
6386000
6384000
6382000
6380000
6378000
Y-axis
X-axis

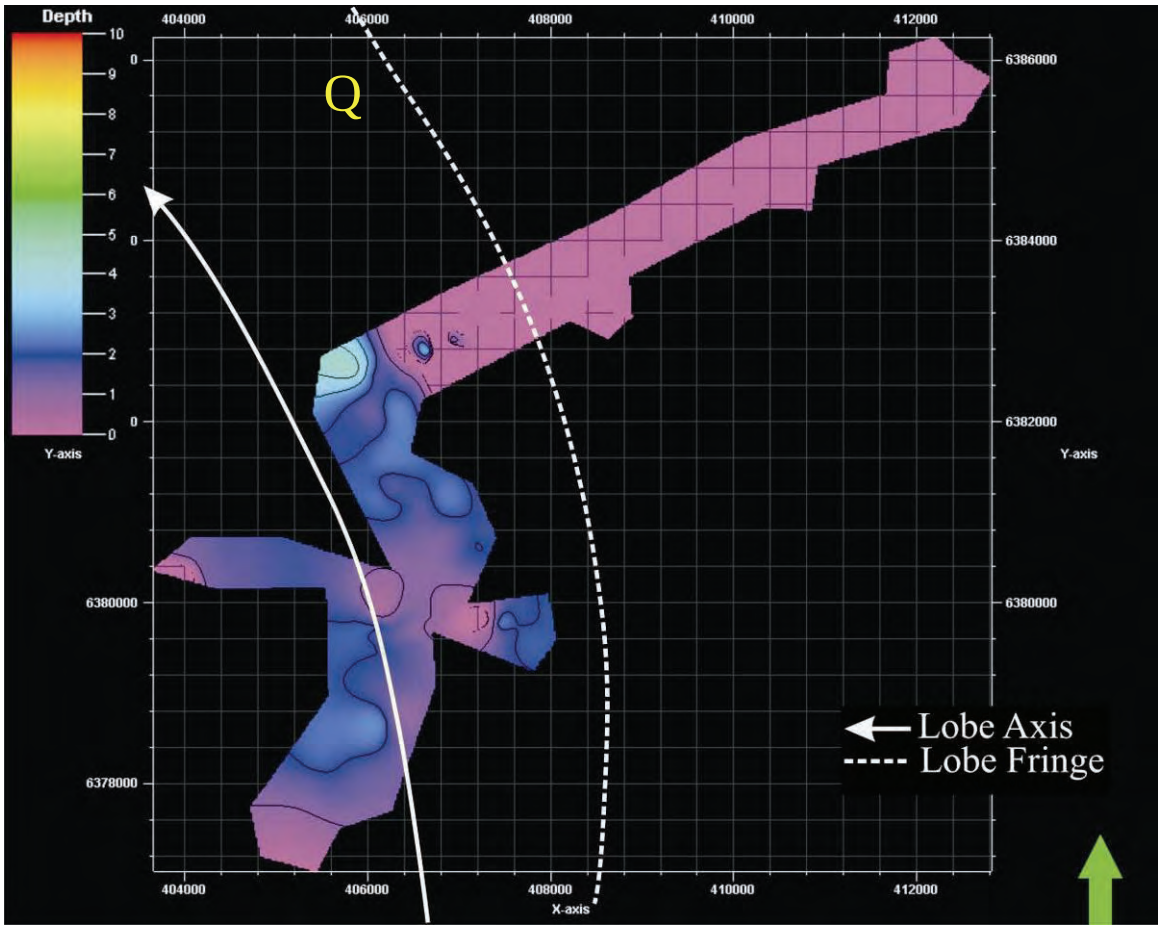
Depth
10
9
8
7
6
5
4
3
2
1
0
Y-axis
Q
404000
406000
408000
410000
412000
6386000
6384000
6382000
6380000
6378000
X-axis
Lobe Axis
Lobe Fringe

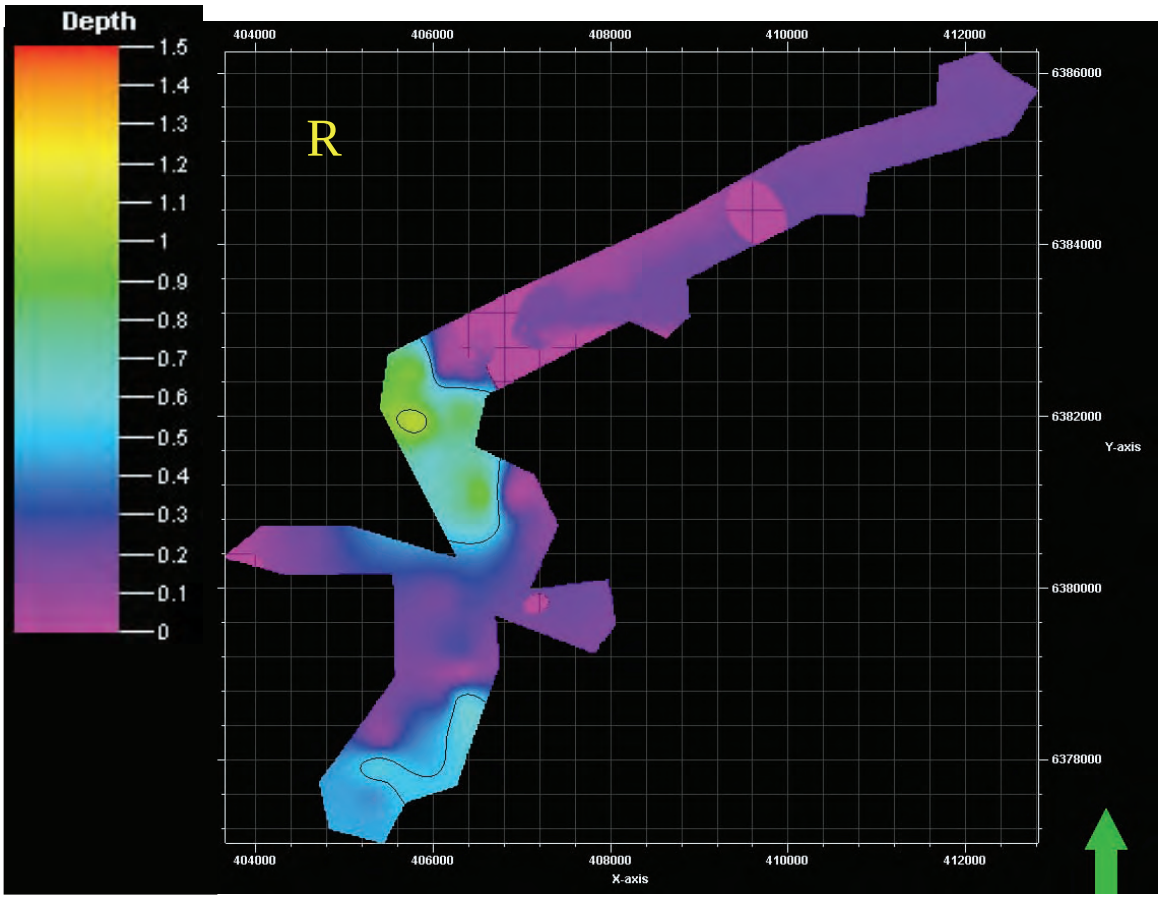
Depth
1.5
1.4
1.3
1.2
1.1
1
0.9
0.8
0.7
0.6
0.5
0.4
0.3
0.2
0.1
0
R
404000
406000
408000
410000
412000
6386000
6384000
6382000
6380000
6378000
Y-axis
X-axis

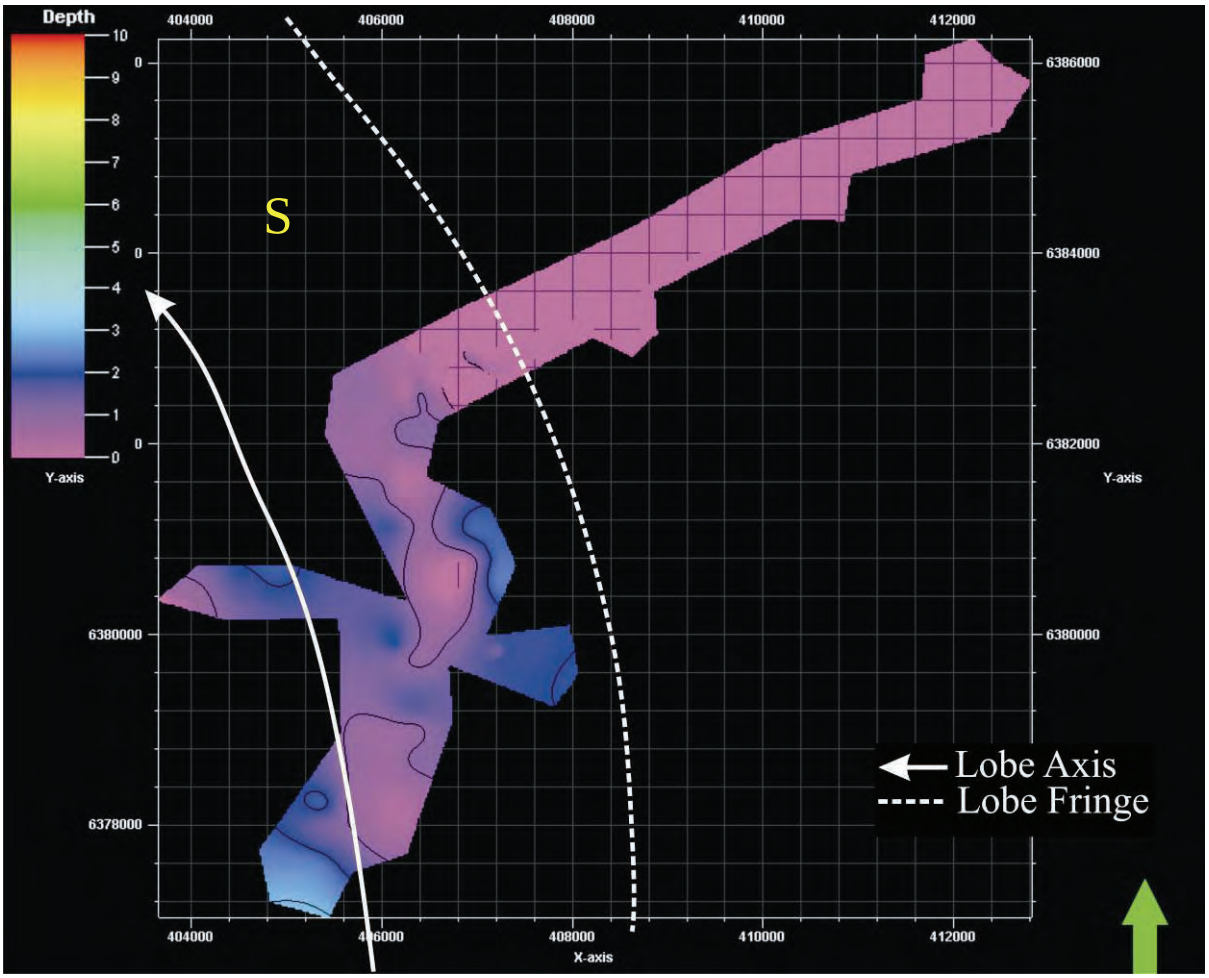

Figure C.2 The final set of Thickness Maps.

Figure C.2 Legend

A - Lobe 6
B - Interlobe F
C - Upper Lobe 5
D - Intralobe 4
E - Lower Lobe 5
F - Interlobe E
G - Upper Lobe 4
H - Intralobe 3
I - Lower Lobe 4
J - Interlobe C and D
K - Upper Lobe 2
L - Intralobe 2
M - Lower Lobe 2
N - Interlobe B
O- Lobe 1
P - Interlobe A
Q - Sub Lobe 2
R - Intralobe 1
S - Sub Lobe 1

Appendix D

Petrel Correlation Panels

Petrel Correlation Panels

The Panels presented here were created using Petrel's correlation function. They display the same wells as the corresponding Panels in Appendix A. The difference is of course the correlations themselves: they are represented by the calculated well-tops, and are not manually inserted. Figure D.1 is a representation of the first few wells in the Gemsbok River valley (starting with J0000000LK), but here the first Kriging surfaces are also included to show the lack of accuracy. When up-scaling a well, everything not situated between two surfaces is omitted, and therefore lost to later work.

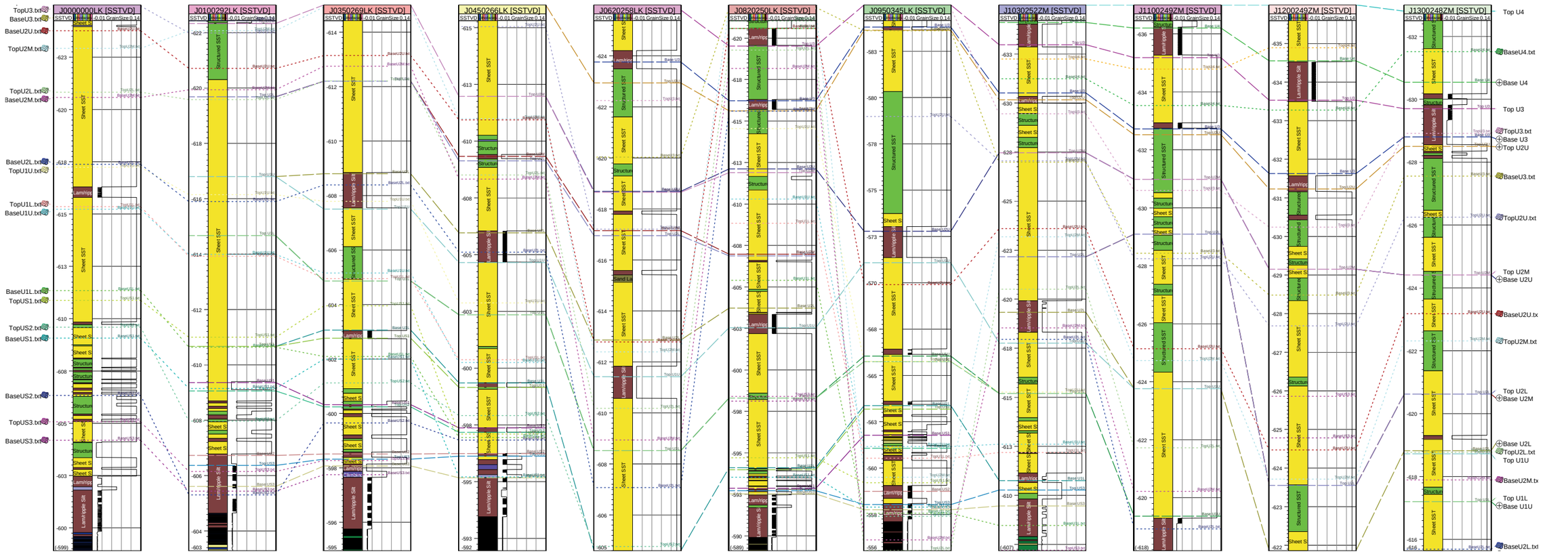

Figure D.1 An example correlation panel created in Petrel, showing both the original DSL facies as well as the grain size. Both the well-tops (dashed lines) and the surfaces (dotted lines) created with the Kriging algorithm are included. Note the mess. The well-tops are at the correct levels, whereas the surfaces are literally all over the place. This is what prompted the use of a different algorithm, as the results gained with Kriging simply weren't useful.

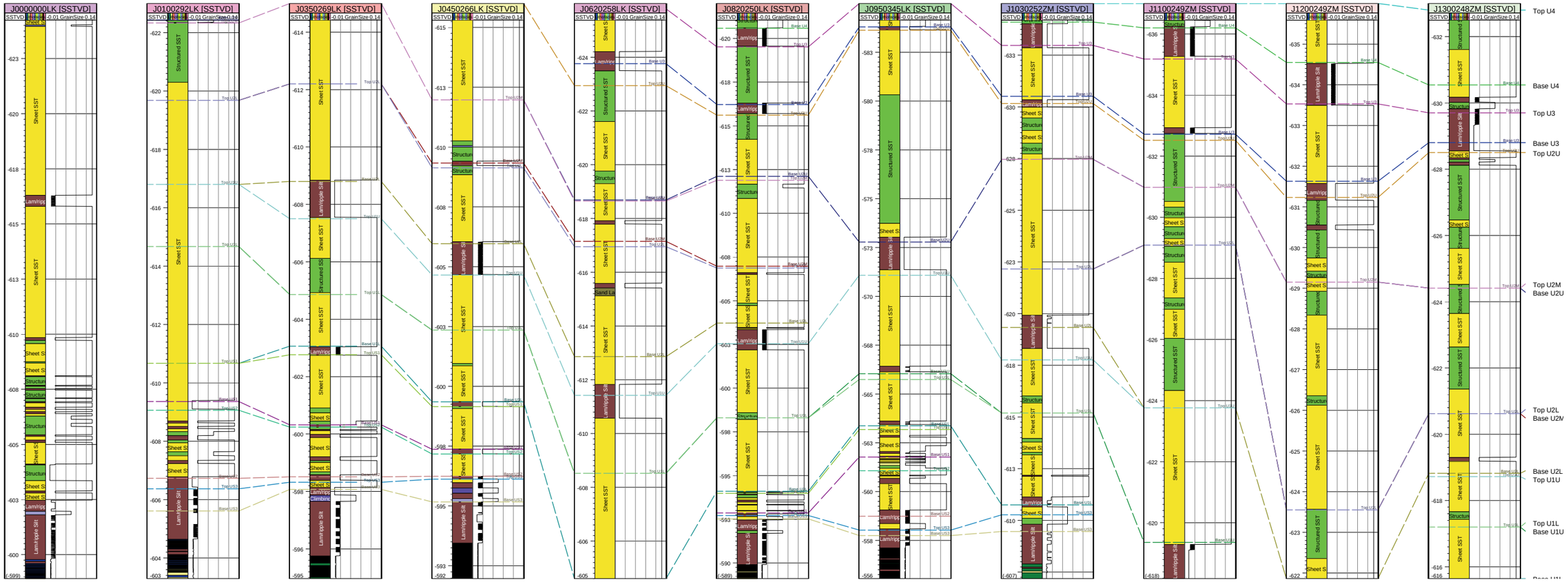

Figure D.2 The same correlation as in figure D.1, only this time the surfaces were omited in order to give a clear representation.

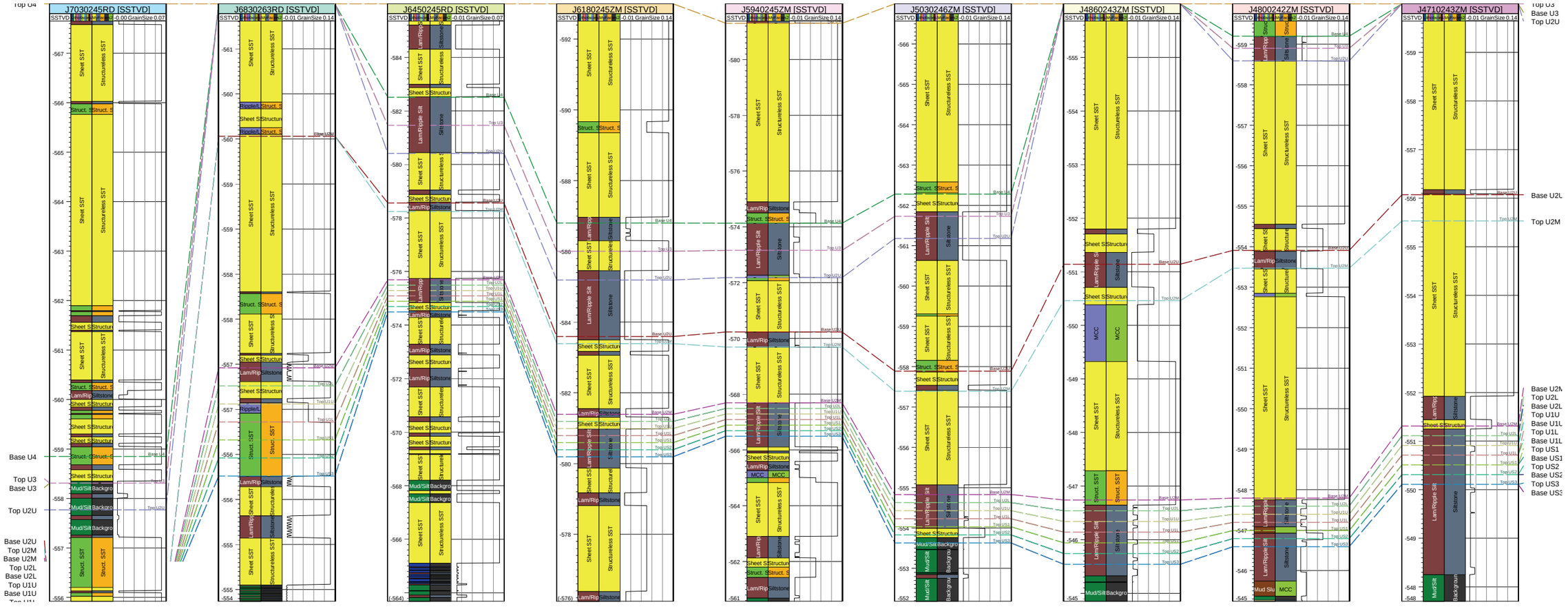

Figure D.3 Panel 1 - 2 as represented by Petrel. Here the new facies as well as the new Excel data is represented. This view in 2D provides a much clearer picture of what the "new" data achieved by extending "missing" units to the full length of the field area.

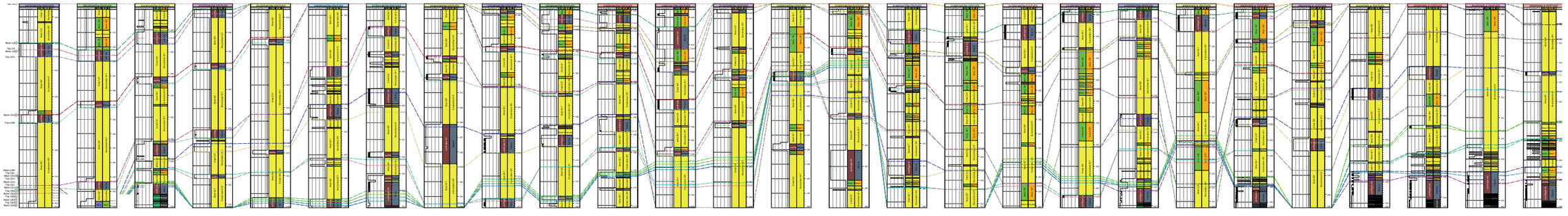

Figure D.4 Panel 3 as represented by Petrel.

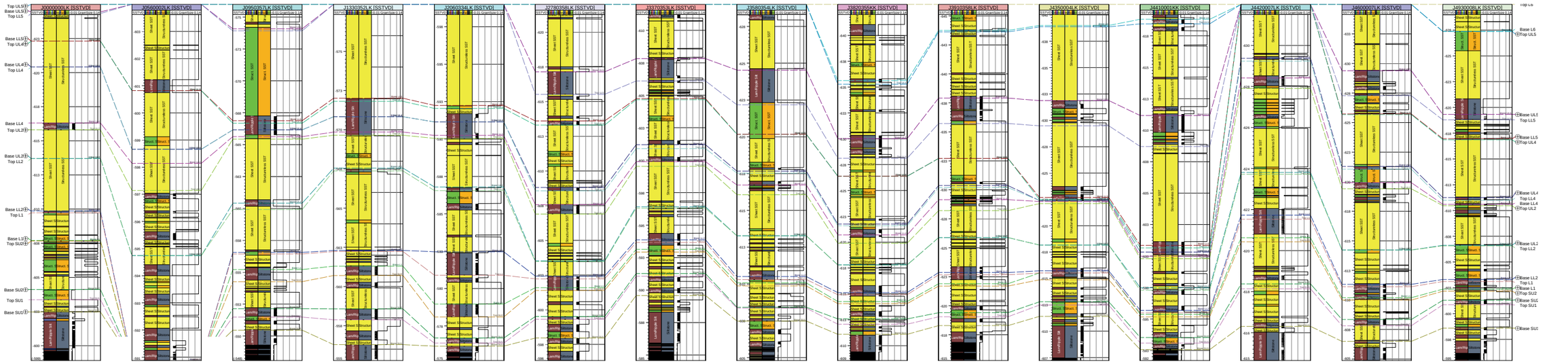

Figure D.5 Panel 12 as represented by Petrel

Appendix E

Interpolation Algorithms in Petrel

Interpolation Algorithms in Petrel

(based on descriptions in Petrel Online Help)

There are numerous algorithms included in Petrel which can be used to create surfaces and interpolate models, and by extension, grids used for models, which are also surfaces. Some of these are: closest, artificial, moving average, directional trend, functional, cos expansion, convergent gridder, Kriging, and sequential Gaussian simulation.

This appendix is a short summary of some of the algorithms used in Petrel, as described in the Online Help files of Petrel 2007.1.2.

Closest algorithms use the closest input point for the creation of surfaces.

Artificial algorithms can use five different methods, all based on variation, or lack thereof, of Z-values. The Z-values can either be constant, or based on complex variation from sources such as isochors. The dip and azimuth can also be defined for some methods.

Moving average algorithms find an average of the input data and weights it according to its distance from data points. The algorithm is fast and will create values for all cells of a grid. It can, however, create concentric patterns if the range of the input data is large. The algorithm will not generate values larger or smaller than the minimum and maximum values of the input data. Petrel can utilise the algorithm by changing the exponent.

Directional trend algorithms are not so much used for surface creation as to give a directional trend to any other algorithm used for interpolation. Both the direction and influence weight can be adjusted.

Functional algorithms use standard equations, from straight lines to parabolic functions, to create 3-dimensional functions. It then uses these functions in the interpolation of Z-values for a surface. The algorithm weights the input points by distance and will be recalculated for each interpolation. It will keep a trend going, and is therefore best suited for twenty or more input points. The algorithm actually requires more than a few points so as not to fail.

Cos expansion algorithms create smooth surfaces, in other words it minimizes curvature. This is useful for few points, but cumbersome when points become too numerous, and can fail if points are too close together.

Convergent gridder algorithms are control point orientated algorithms (as opposed to grid point) which will converge upon the solution iteratively adding more and more resolution. The result is that general trends are retained even in areas with little data, while detail is honoured in areas where the data exists. This algorithm is the surface gridding and smoothing algorithm used

when building a structural model, a single surface model or smoothing a grid. A general-purpose algorithm, it is suited to a variety of data types of various densities. It can handle line data (such as fault interpretations), dense data point distributions (horizon interpretation grids), sparse data point distribution (horizon marker interpretations), or a combinations of the above, as well as other data types. It can honour data approximately (geophysical data) or exactly (geologic data). The algorithm is fast, building the model in stages by iterating or converging from an initial to a final solution. There is no data searching or sorting. The iterative converging process ensures this is a data-driven process which requires minimal parameter control, although many parameters are available. Surface derivatives at every iteration are interpolated and fed into the next iteration. Extrapolation is stable, even at large distances from the data.

Kriging algorithms use variograms to express the spatial variability of the input data (variograms are used to analyse the spatial variation of reservoir properties, and are based on the principle that closely spaced data are more likely to correlate than data spaced farther apart, and after a certain distance a minimum correlation is reached, after which distance becomes irrelevant). The type of function for the variogram, namely exponential, spherical and Gaussian, range, sill and nugget can all be defined manually. The algorithm will not generate values larger or smaller than the minimum and maximum values of the input data.

The **Sequential Gaussian simulation** is a stochastic method of interpolation based on Kriging. It is capable of honouring input data, input distributions, variograms and trends. During the simulation, local highs and lows will be generated between input data point locations which honour the variogram, the positions of which will be determined by a random number which can be set manually, but in the absence of other information, the input distribution will be given by the original input data. In the latter case the result will not produce values above or below the maximum and minimum of the input data.